Biochimica et Biophysica Acta 1848 (2015) 392–407

Contents lists available at ScienceDirect

Biochimica et Biophysica Acta

journal homepage: www.elsevier.com/locate/bbamem

Surface behavior of peptides from E1 GBV-C protein: Interaction with anionic model membranes and importance in HIV-1 FP inhibition

R. Galatola [b], A. Cruz [c], M.J. Gómara [b], J. Prat [a,b], M.A. Alsina [a], I. Haro [b], M. Pujol [a,*]

[a] Physical Chemistry Department, Faculty of Pharmacy, University of Barcelona, CSIC-Associated Unit: Peptides and Proteins: Physicochemical Studies, IN2UB Av. Joan XXIII s/n, 08028 Barcelona, Spain
[b] Unit of Synthesis and Biomedical Application of Peptides, Department of Biomedical Chemistry, IQAC-CSIC, Jordi Girona 18, 08034, Barcelona, Spain
[c] Dept. de Bioquímica y Biología Molecular I, Facultad de Biología, Universidad Complutense, 28040 Madrid, Spain

ARTICLE INFO

Article history:
Received 10 May 2014
Received in revised form 20 October 2014
Accepted 21 October 2014
Available online 30 October 2014

Keywords:
GBV-C peptide
HIV-1 FP
Lipid model membrane
Fluorescence technique
AFM
Hemolysis

ABSTRACT

The interaction between a peptide sequence from GB virus C E1 protein (E1P8) and its structural analogs (E1P8-12), (E1P8-13), and (E1P8-21) with anionic lipid membranes (POPG vesicles and POPG, DPPG or DPPC/DPPG (2:1) monolayers) and their association with HIV-1 fusion peptide (HIV-1 FP) inhibition at the membrane level were studied using biophysical methods. All peptides showed surface activity but leakage experiments in vesicles as well as insertion kinetics in monolayers and lipid/peptide miscibility indicated a low level of interaction: neither E1P8 nor its analogs induced the release of vesicular content and the exclusion pressure values (π_e) were clearly lower than the biological membrane pressure (24–30 mN m^{-1}) and the HIV-1 FP (35 mN m^{-1}). Miscibility was elucidated in terms of the additivity rule and excess free energy of mixing (G^E). E1P8, E1P8-12 and E1P8-21 (but not E1P8-13) induced expansion of the POPG monolayer. The mixing process is not thermodynamically favored as the positive G^E values indicate. To determine how E1 peptides interfere in the action of HIV-1 FP at the membrane level, mixed monolayers of HIV-1 FP/E1 peptides (2:1) and POPG were obtained. E1P8 and its derivative E1P8-21 showed the greatest HIV-1 FP inhibition. The LC-LE phase lipid behavior was morphologically examined via fluorescence microscopy (FM) and atomic force microscopy (AFM). Images revealed that the E1 peptides modify HIV-1 FP–lipid interaction. This fact may be attributed to a peptide/peptide interaction as indicated by AFM results. Finally, hemolysis assay demonstrated that E1 peptides inhibit HIV-1 FP activity.

1. Introduction

Recent years have seen the publication of numerous studies in which co-infection with GB virus C (GBV-C) and HIV-1 has been associated with slower progression of the illness and a higher survival rate of patients once AIDS has developed [1–3]. These two viruses share transmission routes and thus co-infection is common [4].

Several studies have been published to propose different models of interaction between GBV-C and HIV-1 virus [5]. One of the proposed mechanisms by which GBV-C modulates HIV-1 infection and AIDS progression involves inhibiting HIV-1 replication *in vitro* by GBV-C proteins [6–9]. Based on single cycle replication studies, E2 and NS5A viral proteins inhibit HIV-1 at least in part at the HIV-1 entry step. The GBV-C E2 protein directly inhibits HIV-1 pseudovirus entry, and peptides derived from the E2 protein interfere with HIV-1 cellular binding and fusion, independent of the viral effect on CD4 cell homeostasis [6,7]. In contrast, NS5A protein expression down regulates CXCR4 surface expression and induces the release of the CXCR4 ligand (SDF-1) in CD4 + T cells [8,9]. GBV-C NS5A protein also decreases CD4 surface expression via a reduction in steady state CD4 mRNA levels [10].

In our hands, certain 18-mer peptide sequences of the E2 envelope protein of the GBV-C notably decrease cellular membrane fusion and interfere with HIV-1 infectivity, highlighting their potential utility in future anti-HIV-1 therapies [11]. Furthermore, synthetic peptides derived from GBV-C E1 protein also inhibit HIV-1 entry and appear to interact with HIV-1 FP [12–17].

Based on these findings, the sequence E1 (22–39) of GBV-C protein (E1P8) was selected [14,16,17] in order to better analyze its interaction with HIV-1 FP. We studied the influence of each amino acid residue on the primary structure and the total net charge of the peptide. Firstly, we replaced each amino acid in the sequence with Ala and replaced charged residues with neutral amino acids [18]. Then the E1 peptide analogs were evaluated with regard to their capacity to inhibit the destabilization process of POPG unilamellar lipid vesicles induced by HIV-1 FP [18]. Three derivatives of GBV-C E1P8 (E1P8-12, E1P8-13 and E1P8-21) were selected on the basis of a higher effect relative to the parent peptide E1P8 in terms of decreasing the leakage of vesicular content induced by HIV-1 FP [18].

* Corresponding author. Tel.: +34 93 403 35 57; fax: +34 93 403 59 87.
E-mail address: mopujol@ub.edu (M. Pujol).

http://dx.doi.org/10.1016/j.bbamem.2014.10.033
0005-2736/

The most important processes, which occur in the cellular level, such as viral infection or neurotransmission for instance, take place through the membrane. The membrane models are used frequently to understand these processes. It is known that HIV-1 FP interacts more with negatively charged lipids than zwitterionic lipids [19]. In this work, to mimetize the negative charge feature, anionic phospholipids POPG (1-palmitoyl-2-oleoyl-sn-glycero-3-phospho-rac-(1-glycerol) and DPPG (1,2-dipalmitoyl-sn-glycero-3-phophoglycerol) and a mixture of DPPC (1,2-dipalmitoyl-*sn*-glycero-3-phosphocholine) and DPPG (2:1) were chosen. As model membranes, POPG unilamelar vesicles were used for leakage studies; POPG monolayers to characterize thermodynamically peptide–lipid interactions and the peptide insertion in the lipid monolayer; DPPG to obtain Langmuir–Blodgett films for fluorescence microscopy (FM) in order to analyze the effect on lipid phase transition. To realize the lipid–peptide and peptide–peptide interaction a molecular level, a mixture of DPPC/DPPG (2:1) that resembles better the negative charge ratio in biological membranes, was used to obtain Langmuir–Blodgett films on mica substrate for AFM imaging studies. Finally, we performed hemolysis assays with rabbit cells in order to confirm peptides activity *in vivo*.

2. Materials and methods

2.1. Materials

1-Palmitoyl-2-oleoyl-sn-glycero-3-phospho-rac-(1-glycerol) (POPG), 1-palmitoyl-2-{6-[(7-nitro-2-1,3-benzoxadiazol-4-yl)amino] hexanoyl}-sn-glycero-3-phosphocoline (NBD-PC), 1,2-dipalmitoyl-sn-glycero-3-phophoglycerol (DPPG) and 1,2-dipalmitoyl-*sn*-glycero-3-phosphocholine (DPPC) were purchased from Avanti Polar Lipids.

Chloroform and methanol were purchased from Merck. Double distilled and deionized water was used (18.2 MΩcm, pH 5.8) (MilliQ system, Millipore). Hepes (Sigma-Aldrich) 5 mM and NaCl (Carlo Erba) 20 mM were used to make a buffer solution, pH 7.4. PBS buffer 0.1 M was prepared with 120 mM NaCl, 2.7 mM KCl and 10 mM Na_2HPO_4 (Merck).

2.2. Peptide synthesis

The E1P8 peptide (APEDIGFCLEGGCLVALG) corresponding to E1 protein of GBV-C) and its derived analogs E1P8-12, E1P8-13 and E1P8-21, were synthesized via solid-phase peptide methodology following a 9-fluorenylmethoxycarbonyl (Fmoc) strategy by means of DIEA/HATU activation.

HIV-1 FP was synthesized in the same way but using a polyethylene glycol-based resin, ChemMatrix, via solid phase methodology as described previously [11].

Crude peptides were desalted using an Oasis HLB Plus cartridge 225 mg/60 μg from Waters. These cartridges contain a polymeric water-wettable reversed phase sorbent.

The final characterization of synthetic peptides was carried out via analytical HPLC and electrospray mass spectrometry.

2.3. Surface activity of peptides

The experiments were carried out on a NIMA Langmuir Balance (Coventry, UK) at 297 ± 1 K. Using a cylindrical PTFE trough (19.6 cm^2, 30 ml), increasing volumes of E1P8, E1P8-12, E1P8-13, and E1P8-21 peptide solution (1 mg ml^{-1} in acetonitrile/H_2O) were injected below the Hepes subphase (pH 7.4) through a lateral hole. The subphase was stirred continuously with a miniature Teflon-coated spinning rod. Surface pressure, π, was monitored with an accuracy of ±0.05 mN m^{-1} using a platinum plate as the pressure sensor.

2.4. Penetration kinetics

The kinetics of insertion of the peptides into monolayers of POPG was measured using the same trough as for the surface activity. Lipids from a concentrated solution (1 mg ml^{-1} in chloroform) were spread at the air/water interface until the desired lipid surface pressure (π_i) was achieved. Once the lipid monolayer had equilibrated, a 0.38 μM peptide solution was injected into the Hepes subphase through the side hole of the trough. The subphase was magnetically stirred during the measurements, and surface pressure changes were monitored as a function of time until pressure remained constant. The experiment was carried out at 297 ± 1 K.

2.5. Compression isotherms

Compression isotherms were performed at room temperature (297 ± 1 K) in a NIMA Langmuir Teflon trough (surface area 690 cm^2, volume 350 ml) containing Hepes 5 mM pH 7.4. Lipids were dissolved in chloroform (1 mg ml^{-1}). Pure peptide monolayers (1 mg ml^{-1}) were formed by direct spreading from DMSO (5%)/chloroform solution using a microsyringe. Mixed monolayers were obtained by premixing lipid/peptides in the desired proportions, and then directly spreading on the surface. The spreading solvent was allowed to evaporate for at least 10 min before compression started, at a rate of 5 cm^2 min^{-1}.

2.6. Fluorescence microscopy

Surface pressure-area measurements were performed using a NIMA Langmuir–Blodgett trough (surface area 200 cm^2) equipped with a continuous Teflon-ribbon barrier able to sustain maximal surface pressures with no leakage, and thermostated at the desired temperature (297 ± 1 K). The trough was set inside a custom-made closed chamber to ensure isolation from external light.

The phospholipid DPPG (1 mM), containing 1 mol% of NBD-PC, and its mixtures with peptides (5% with respect to phospholipid, mol/mol) were prepared in chloroform/methanol (2:1 v/v). Monolayers were formed by applying small drops of the spreading solution on the water subphase. After 10 min, Langmuir–Blodgett films were prepared using the COVASP method [19,20]. Briefly, as Wang et al. described [19], in this method the monolayers were compressed at 25 cm^2 min^{-1} along the pressure-area isotherms while simultaneously being transferred onto a Menzel-Glaser 24 mm × 60 mm cover slips at a rate of substrate movement of 5 cm^2 min^{-1}. The entire transferred film typically occupied a length of ~20 mm on the substrate. π-A compression isotherms were simultaneously recorded during the transfer. This technique permits capture of all the structural features shown by a given film along the whole compression isotherm in a single supported layer (termed continuously varying surface pressure (COVASP) films).

The transferred monolayers were observed in a Leica DM4000B microscope (Leica Microsystems, Wetzlar, Germany) equipped with appropriate fluorescence filters to allow for the observation of NBD-PC fluorescence (maximum fluorescence excitation at 480 nm and emission at 526 nm). Images of the transferred films were obtained at different positions and subsequently assigned to the surface pressures obtained during film transfer [19].

2.7. AFM measurements

AFM intermittent contact mode images in air were obtained using a Nanoscape IV Multimode AFM (Bruker AXS Corporation, Madison, WI) with MSNL silicon tips with a nominal spring constant of 30 pN nm^{-1}. To minimize the applied force on the sample, the set point was continuously adjusted during imaging. Images were acquired at 0° scan angle at 1.5 Hz of scan rate. All images were processed using Bruker and Image software.

2.8. Leakage of vesicular contents: ANTS/DPX assay

For the leakage assay [21,22], unilamellar lipid vesicles (LUVs) of POPG containing fluorescent probes ANTS (8-aminonaphtalene-1,3,6-trisulfonic acid) and DPX (N,N′-p-xylene-bis(pyridinium bromide) in Hepes buffer (5 mM, pH 7.4) were prepared according to a previously described protocol [23].

The peptides dissolved in DMSO were added to the suspension 0.1 mM of LUVs, and the fluorescence was measured in a PTI QM4CW spectrofluorimeter (at room temperature) before and after detergent was added. The dequenching of coencapsulated ANTS and DPX fluorescence resulting from dilution was measured to assess the leakage of aqueous contents from vesicles. Leakage was monitored by measuring the increase in the ANTS/DPX fluorescence intensity at 520 nm, with an excitation of 355 nm. The peptide/LUVs molar ratio was 1/3. The percentage of leakage was calculated according to the equation: $\%\text{leakage} = [(F - F_0)/(F_{100} - F_0)] \times 100$, in which F_0 is the initial fluorescence of LUVs, F is the fluorescence intensity after adding the peptide, and F_{100} is the fluorescence intensity after the addition of 10 μl of a 10% (v/v) Triton 100 solution (complete lysis of LUVs).

2.9. Hemolysis assay

The effect of E1P8 peptide and its analogs (E1P8-12, E1P8-13 and E1P8-21) on red blood cell destabilization promoted by the presence of HIV-1 FP was determined after incubation of different concentrations of the E1P8 peptides with diluted suspensions of cells.

Rabbit blood samples were extracted immediately before use. Erythrocytes were centrifuged for 10 min at 1000*g*. The supernatant was discarded and the pellet was washed three times with PBS. Red blood cells were then diluted 1:10 in PBS.

Stock solutions of 2 mM HIV-1 FP and 20 mM of the parent peptide and its analogs were prepared in DMSO. E1P8, E1P8-12, E1P8-12 and E1P8-21 peptide aliquots ranging between 0 and 1000 μM were distributed in tubes. Thereafter, 2 mM of HIV-1 FP solution in PBS was added, resulting in a final HIV-1 FP concentration of 100 μM. After 60 min at 310 K, 10% of the erythrocytes were added and incubated for another 60 min at 310 K. Each sample was prepared and analyzed in triplicate. Thereafter, cells were pelleted for 5 min at 1000*g*. Supernatants were transferred to 96-MicroWell™ Solid Plates and optical density was measured at 405 nm. Percent hemolysis values were expressed relative to the total hemolysis caused by the respective HIV-1 FP alone.

3. Results and discussion

3.1. Surface activity of peptides

Surface activity experiments provide information about the capacity of a peptide to adsorb or incorporate into the air-buffered interface.

The adsorption kinetics of E1P8 and its analogs (E1P8-12, E1P8-13 and E1P8-21) was measured by injecting increasing volumes of a concentrated peptide solution into a Hepes subphase and recording the surface pressure achieved as a function of time at a constant area. The experiments were carried out for more than 2 h in every case, but after 100 min the pressure remained constant, and we considered the equilibrium to have been reached by this time.

For each peptide studied a slight gradual adsorption of peptide was observed at low concentrations. The higher the peptide concentration in the subphase, the faster the incorporation and the higher the surface pressure achieved. Fig. 1 illustrates the adsorption isotherm profile for the parent peptide and its analogs. The surface activity curve was fitted via non-linear least-squares regression analysis, revealing a rectangular hyperbola $\Delta\pi = (c\pi_{max})/(K + c)$, where c is the peptide concentration, π_{max} is the maximum surface pressure achieved and K is a characteristic constant equal to the peptide concentration that reaches half π_{max}. The characteristic physicochemical parameters obtained for each peptide

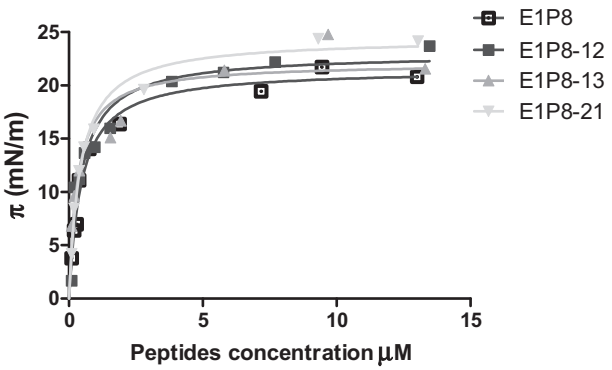

Fig. 1. Surface activity curve of E1P8 and its analogues peptides.

are shown in Table 1. K values were frequently chosen for further penetration studies, as K corresponds to the concentration of peptide that should be used in the bulk subphase for experiments of penetration kinetics, being lower than the equilibrium spreading pressure of the peptide [24,25]. In our case, a different K value was found for each peptide. In the kinetics experiments, in order to compare the behavior of peptides, we used the same concentration in each case, 0.38 μM, as it corresponds to the value of each peptide prior to reaching the equilibrium spreading pressure.

Analysis of the peptide adsorption process from the subphase to the air–water interface allows the calculation of the peptide surface excess concentration (Γ) by applying the Gibbs adsorption equation $\Gamma = (1/RT)(d\pi/d\ln c)$, where R is the gas constant (8,31 J K^{-1} mol), T is the temperature (297 ± 1 K), $(d\pi/d\ln c)$ is the slope of a plot of surface pressure achieved for each peptide concentration in front of the logarithm of peptide concentration [13]. Using peptide maximum surface excess concentration it is possible to calculate the molecular area ($Area = 1/N\Gamma_{max}$, where N is Avogadro's constant). The results are shown in Table 1.

The shape of the adsorption isotherms of the analogs was similar to those of the parent peptide, with parameters of the same order of magnitude as those found for other peptide sequences [14,26–29]. The hydrophobic profile based on their primary sequence clearly induced an increase in surface pressure at the air–water interface when they were injected into the subphase. Their high hydrophobicity profile was confirmed by the Hopp–Woods scale [30]. In this type of plot, values lower than 0 are hydrophobic. Fig. 2 shows the Hopp–Woods profile of GBV-C E1P8 protein. The red arrows indicate the E1P8 sequence. According to previous study [14], it can be seen the hydrophobic character of this peptide. The analogs present the same hydrophobic profile, and for this reason the surface activity is the same. Consequently, the surface parameters of each peptide were similar (Table 1), including the maximum pressure achieved by peptides (between 22 and 24 mN m^{-1}) and the area per molecule (A) (between 1.04 and 1.12 nm^2 mol^{-1}). E1P8-13 showed lower values of constant (K) and the surface excess concentration at equilibrium.

Table 1
Analysis of the adsorption isotherms of parent peptide E1P8 and its analogues E1P8-12, E1P8-13, E1P8-21. π_{max} is the maximum surface pressure achieved and K is a characteristic constant equal to the peptide concentration that yields (1/2) π_{max}. Γ_{max} is the maximum surface excess concentration at equilibrium and A is the molecular area.

	π_{max} (mN m^{-1})	K (μM)	Γ_{max} (mol m^{-2})	A (nm^2 mol^{-1})
E1P8	22	0.45	1.53×10^{-6}	1.06
E1P8-12	23	0.44	1.59×10^{-6}	1.04
E1P8-13	22	0.32	1.48×10^{-6}	1.12
E1P8-21	24	0.42	1.52×10^{-6}	1.09

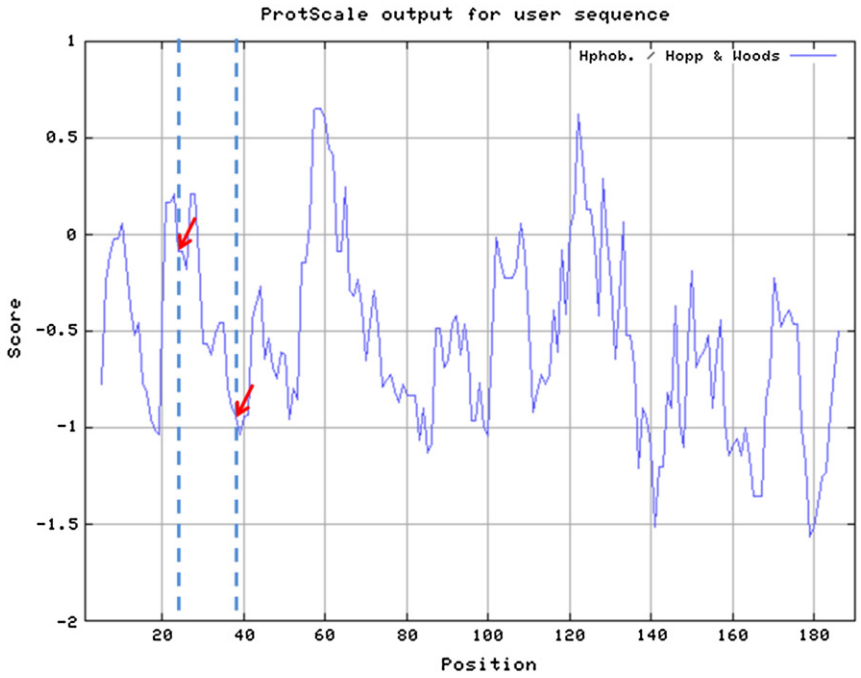

Fig. 2. Hoop and Woods profile for GBV-C E1 protein obtained by Expasy software (http://web.expasy.org/protscale/). Red arrows show the region where the E1 (22–39) peptide sequence (E1P8) is located.

3.2. Lipid–peptide interaction

3.2.1. Leakage of vesicular contents: ANTS/DPX assay

The sequence E1P8 of the GBV protein and its derivative sequences E1P8-12, E1P8-13 and E1P8-21 were evaluated with regard to their capacity to induce the destabilization of lipid vesicles of POPG. Thus, the effect of the peptides on the release of the encapsulated fluorophores ANTS/DPX was monitored by dequenching of the ANTS. The peptides were dissolved in DMSO before addition to the liposome suspension, after which the emission of the ANTS probe was recorded at 520 nm. The trials were performed in a PTI QM4CW spectrofluorimeter, in 96-well plates. The fluorescence assay was carried out in triplicate and repeated twice on different days to analyze intra- and inter-assay fluorescence variations. HIV-1 FP was used as a control peptide in this assay. HIV-1 FP interacts with negatively charged phospholipids and induces leakage from large unilamellar phospholipids of POPG [11,31].

Fig. 3 shows the percentage of leakage of LUVs induced by HIV-1 FP, E1P8, E1P8-12, E1P8-13 and E1P8-21. Neither E1P8 nor its analogs induced the release of vesicular contents.

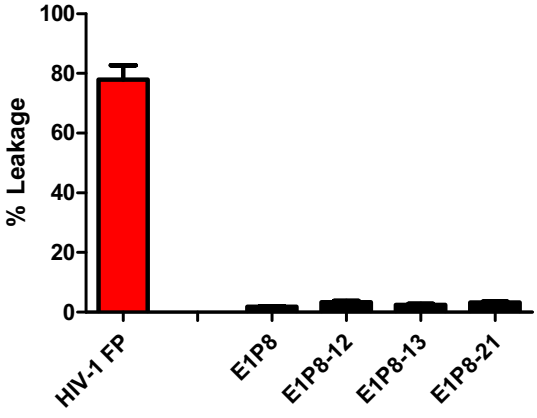

Fig. 3. % Leakage of POPG LUVs induced by HIV-1 FP, E1P8, E1P8-12, E1P8-13 and E1P8-21.

3.2.2. Penetration kinetics

Membrane peptide affinity can be determined by measuring the exclusion pressure of insertion [32–34]. The exclusion pressure, π_e, which is the lipid monolayer surface pressure above which the peptide does not penetrate into the monolayer, can be determined from the plot of the initial lipid pressure (π_i) as a function of surface pressure increase ($\Delta\pi$) by extrapolating the plot at $\Delta\pi$ = zero [35]. If a monolayer of phospholipid is prepared at the air/water interface at a certain surface pressure and a peptide is injected below the monolayer, the lipid film surface pressure would increase as peptide molecules bind to or insert into the lipid monolayer at constant surface area [23,32]. The degree of surface pressure increase depends on the type of lipid, initial film surface pressure, peptide surface activity, and concentration used. Furthermore, given that the membrane lateral surface pressure has been estimated to range between 25 and 35 mN m^{-1} [36,37], lower values indicate a low level of interaction with the membrane.

The ability of E1P8 and its analogs E1P8-12, E1P8-13 and E1P8-21 to insert into POPG anionic phospholipid monolayers spread through the air–water interface was monitored by measuring variations in surface pressure using different initial surface pressures of POPG, and by

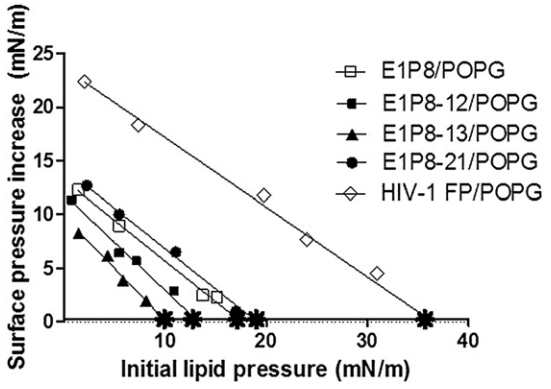

Fig. 4. Surface pressure increase ($\Delta\pi$) caused by HIV-1 FP, E1P8 and its analogues E1P8-12, E1P8-13, E1P8-21 in monolayers of POPG in front of the lipid initial pressure (π_i). Points * indicate π_e of peptides from monolayer.

injecting a given peptide concentration into the subphase (Hepes 5 mM pH 7.4). The selected concentration corresponds to the concentration prior to saturation (0.38 μM).

A linear plot of $\Delta\pi$ versus π_i was obtained for each peptide (Fig. 4). The greater the π_i the lower the incorporation of the peptide into the monolayer because of the closer packing of the lipids at higher initial surface pressure.

Table 2 shows the net charge of the peptides and the exclusion pressure for E1P8, E1P8-12, E1P8-13 and E1P8-21; at this surface pressure the POPG monolayer is in an expanded state, as described in the section below, such that the peptides interact with the lipid through hydrophobic interactions, while the absence of penetration is due to the negative net charge of the peptides. The kinetic penetration of HIV-1 FP was also studied. The HIV-1 FP π_e, which was about 35 mN m^{-1}, demonstrates that this peptide penetrates better than E1P8 and its analogs and interacts with the cellular membrane, presumably due to the positive net charge of HIV-1 FP [29].

3.2.3. Miscibility study

The interaction of E1P8 and its analogs with phospholipid monolayers was also studied in a dynamic system. *π-A* compression isotherms were obtained for pure POPG and changes induced by peptides either in *π-A* isotherm shape or surface compression modulus were analyzed.

The surface compression modulus was calculated according to $C_s^{-1} = -A(\partial\pi/\partial A)_T$, where A is the area per molecule at the indicated surface pressure and π is the corresponding surface pressure. It can be used to characterize the phase state of the monolayer (for liquid expanded films, the monolayer compressibility ranges from 12.5 to 50 mN m^{-1}, while, for the liquid condensed phase, it ranges from 100 to 250 mN m^{-1}) [33,38,39]. Deviations from the additivity rule were also analyzed. These rule predicts that in a two-component system, the area per molecule of the mixture at different mole fractions of each component is a linear combination of the values of the area per molecule for each component multiplied by its mole fraction ($\boldsymbol{A}_{12}^{id} = \boldsymbol{X}_1\boldsymbol{A}_1 + \boldsymbol{X}_2\boldsymbol{A}_2$, where $\boldsymbol{A}_{12}^{id}$ is the mean area per molecule of the mixture of two components, A_1 and A_2 are the area per molecule of the single components at the same surface pressure and X_1 and X_2 are the mole fractions of components 1 and 2 in the mixed film). This is the case when there is either totally ideal mixing or complete immiscibility of the components. In the case that the area per molecule was different from predicted by the additivity rule, the deviations may be positives or negatives. That means the components interact via repulsive or attractive forces respectively [40].

The capacity to form monolayers was studied by performing compression isotherms. Fig. 5 shows the *π-A* compression isotherms of pure monolayers (red line) of E1P8, E1P8-12, E1P8-13 and E1P8-21 and the lipid/peptide mixed films at different molar fractions of components. All formed stable monolayers at the interface. Like other similar peptides [13,15], E1P8 and E1P8-12 exhibited a plateau at the collapse region at 35 mN m^{-1} and 25 mN m^{-1} respectively, which could be the result of the formation of a bilayer [41], or of molecular segments being partially lifted from the water surface [42], or of a change in orientation of the molecules upon compression [43]. E1P8-13 and E1P8-21 monolayers result in a continuously rising isotherm with the collapse pressure at 31 mN m^{-1} and 36 mN m^{-1} respectively.

Table 2
Prediction of the isoelectric point, the net charge at pH 7.4 and the exclusion pressure (π_e) for HIV-1 FP, E1P8 and its derivatives E1P8-12, E1P8-13 and E1P8-21.

	Isoelectric point	Net charge at pH 7.4	Π_e
HIV-1 FP	11.04	1	35
E1P8	2.94	−3.1	17
E1P8-12	2.94	−3	13
E1P8-13	2.94	−3.1	10
E1P8-21	4.04	−1.1	19

The isotherm recorded for pure POPG (black line) showed a monotonous increase in surface pressure until collapse at about 42 mN m^{-1}, which is consistent with data already published; it was noted that the POPG monolayer remained in liquid phase throughout compression (Fig. 5-a inset), as described in previous studies [15,44]. Fig. 5 also shows the mixed lipid/E1 peptide monolayers. Fig. 5-a shows the E1P8/POPG mixed films at different mole fractions. As the amount of E1P8 in the monolayer increased, the pure POPG monolayer expanded, so the area per molecule and Cs^{-1} values shifted to larger and lower values respectively, indicating an increase in membrane fluidity. Plots of area per molecule versus monolayer composition at different surface pressures are shown in Fig. 6-a. These show a slight negative deviation from the additivity rule (see below) at low peptide mole fractions (between 0.2 and 0.4) and also slight positive deviations at peptide mole fractions greater than 0.5. Similar changes were observed in the case of E1P8-12/POPG mixed films (Fig. 5-b), in which as the peptide mole fraction increased the area per molecule values also increased and the Cs^{-1} decreased, making the membrane more compressible. Plots of area per molecule in different mixtures (Fig. 6-b) showed small deviations of ideal behavior mainly at low pressures. Fig. 5-d presents the results obtained for E1P8-21; although it exhibited a similar general trend as E1P8 and E1P8-12 when mixed with POPG, the expansion of pure POPG monolayer was less apparent and the mixtures showed positive deviations from ideality (Fig. 6-d). Finally, in case of E1P8-13 small negative deviations from the additivity rule at low surface pressure were observed in the plot of area per molecule versus monolayer composition (Fig. 6-c), while at higher surface pressure it did not seem to modify the area per molecule of the pure POPG monolayer at any of the peptide mole fractions assayed, but like the other peptides the Cs^{-1} values shifted to lower levels in comparison with the POPG compression modulus.

Concerning collapse pressure, the π_c of E1P8/POPG mixed monolayers shifted to slightly lower values as the peptide mole fraction increased. Pure POPG and pure E1P8 peptide had a similar π_c and only when $x_{E1P8} > 0.6$ did the pseudoplateau appear. In the case of E1P8 derivatives/POPG binary mixtures, mixed films exhibited a gradual decrease in π_c as the $x_{peptide}$ increased. These results are better illustrated by Cs^{-1} analyses (insets of Fig. 5-b, c and d), where the shift in the maximum Cs^{-1} to lower values can be seen. In the case of E1P8-12 the shift in the Cs^{-1} minimum indicating the pressure at which the pseudoplateau appeared is visible along with a second maximum, indicating that E1P8-12 was probably squeezed out of the monolayer upon compression, as when a binary mixture comprises components with different collapse pressures, the resulting isotherm usually exhibits a plateau at a pressure corresponding to the lower π_c of the more fluid component, and a second π_c corresponding to that of the more rigid component [45].

To gain a better insight into the interactions established between POPG with E1P8, E1P8-12, E1P8-13 and E1P8-21, the excess free energy of mixing (G^E) associated with the process was calculated using Eq. (1), as described by Pagano et al. [46], where N_A is Avogadro's number, A_{12} is the mean area per molecule in the mixed film, A_1 and A_2 are the areas per molecule in the pure films, X_1 and X_2 are the molar fractions, and π is the surface pressure (mN m^{-1}).

$$G^E = N_A\left(\int_{\pi\to 0}^{\pi} A_{12}d\pi - \left(X_1\int_{\pi\to 0}^{\pi} A_1 d\pi + X_2\int_{\pi\to 0}^{\pi} A_2 d\pi\right)\right) \quad (1)$$

Table 3 shows the results obtained. The positive values indicate that the process of mixing is not thermodynamically favored and therefore repulsive interactions prevail in the mixtures in comparison with the pure monolayers while negative values indicated that the lipid–peptide interaction are greater than for pure components so, in this case, the process of mixing are favored. In general, low values of $|G^E|$ were observed, all of them lower than the product of RT (2477,5 J mol^{-1}), so according to Gaines et al. [47], the deviations from the additivity

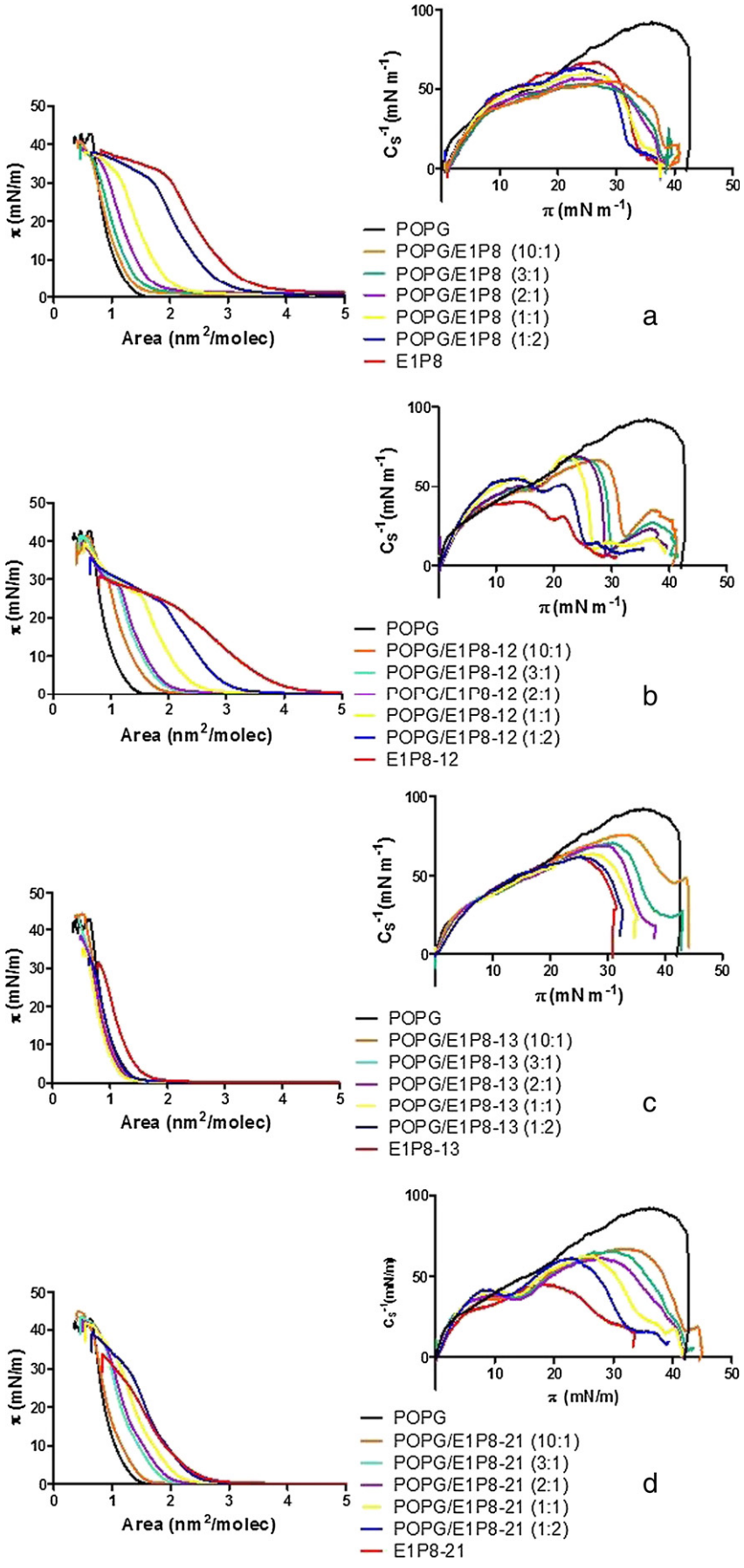

Fig. 5. Surface pressure-mean area per molecule (π-A) compression isotherms for POPG and (a) E1P8, (b) E1P8-12, (c) E1P8-13 and (d) E1P8-21 spread on a Hepes subphase (pH 7.4). Inset: Plots of surface compression modulus ($Cs-1$) as a function of the surface pressure.

rule were not statistically significant and thus the mixtures can be considered totally ideal or not.

3.2.4. Fluorescence microscopy

To analyze the effect of the peptides on the lipid phase-transition, the structure of lipid monolayers at different surface pressures was studied by fluorescence microscopy (FM). As POPG remains in an expanded state during monolayer compression until collapse occurs, a saturated form of PG, DPPG, was used. DPPG has a clear phase-transition from an expanded-liquid to a condensed-liquid state, so the effect of our peptides on this phase transition could be analyzed by transferring the monolayer at variable pressure onto glass cover-slips. Fig. 7 shows the isotherms of DPPG in the absence or presence of 5 mol% of HIV-1 FP, E1P8, E1P8-12, E1P8-13 and E1P8-21. As in the case of POPG, all peptides caused an expansion of the DPPG isotherm to higher areas per molecule, indicating that the peptide was occupying space in the interphase or perturbing the lipid packing. In the presence of HIV-1 FP, the isotherm was similar to that of the monolayer containing only DPPG, with a change in slope close to 30 mN m^{-1} that was not observed in the isotherm of DPPG. At lower pressures the shape of the isotherm presented a plateau associated with the liquid-condensed to liquid-expanded (LC-LE) phase transition of the phospholipid, centered approximately at 5 mN m^{-1}, 2 mN m^{-1} above the transition plateau of DPPG alone [14], according to Cs^{-1} values (Fig. 7-inset).

The behavior of E1P8 and its analogs in DPPG monolayers was more variable. First, a change in the slope of the isotherms was visible at pressures ranging from ~35 mN m^{-1} for E1P8-12 to over 45 mN m^{-1} for isotherms containing E1P8-21. This change in the slope of the isotherm during compression could be associated with changes in the orientation of the peptides in the monolayer or even with partial exclusion of the peptides from the lipid monolayer at higher pressures [48,49]. At lower surface pressures, the monolayers prepared in the presence of E1P8, E1P8-12 and E1P8-21 presented isotherms with a behavior comparable to that of DPPG, appearing to alter the packing rearrangement of DPPG along the phase transition from the LC to LE phases to a lesser extent than HIV-1 FP. However, the DPPG isotherm prepared in the presence of E1P8-13 showed an apparent shift in the phase transition plateau at higher surface pressures (~10 mN m^{-1}) indicating a larger effect on the packaging-rearrangement of DPPG molecules, during the phase transition of the lipid than the other two E1P8 analogs. This delay in the phase transition of DPPG monolayer in the presence of E1P8-13 can be confirmed with Cs^{-1} values (Fig. 7-inset).

To further characterize the effect of the peptides on the lateral phase transition of DPPG, monolayers were prepared in the presence of 1 mol% of the fluorescent dye NBD-PC and were transferred to glass cover slips. The phase transition was visible via fluorescence microscopy (FM) as the appearance of dark domains of condensed phase at the interface that excluded the fluorescent dye. These condensed domains grew in size until the phase transition was complete and they almost completely covered the interface, restricting the fluorescent probe to smaller regions surrounding the LC phase (Fig. 8). Monolayers containing DPPG alone showed a phase transition from LC to LE at 25 °C starting at very low surface pressures of less than 1 mN m^{-1}, and ending above 10 mN m^{-1}.

The addition of the HIV-1 FP peptide to DPPG monolayers induced two clear effects. On the one hand, HIV-1 FP disturbed the lateral phase transition of the lipid, producing larger and more branched domains. In addition, when compared with DPPG images taken at similar pressures, the monolayers containing 5% HIV-1 FP needed to be compressed to higher pressures to complete the transition. While DPPG images showed that almost the entire surface was in the LC phase at 20.4 mN m^{-1}, the monolayers containing 5% HIV-1 FP still showed well-defined domains at 21 mN m^{-1} surrounded by regions that remained in the liquid-expanded phase. HIV-1 FP could thus interact preferentially with the expanded phase of DPPG, preventing the normal growth of LC domains and leading to the formation of branched domains [50]. The heterogeneity in the LE regions observable at relatively low surface pressures (Fig. 8, at 4 mN m^{-1}) could be consistent with the preferential accumulation of HIV-1 FP in this phase. At higher pressures (Fig. 8, at 21 mN m^{-1}) the presence of smaller domains in the LE phase could be due to the formation of new LC regions of DPPG, or even to the lateral segregation of the peptide from the LE phase [14].

When the effect of E1P8 and analog peptides on the phase transition was analyzed, a lesser influence on the DPPG transition phase was

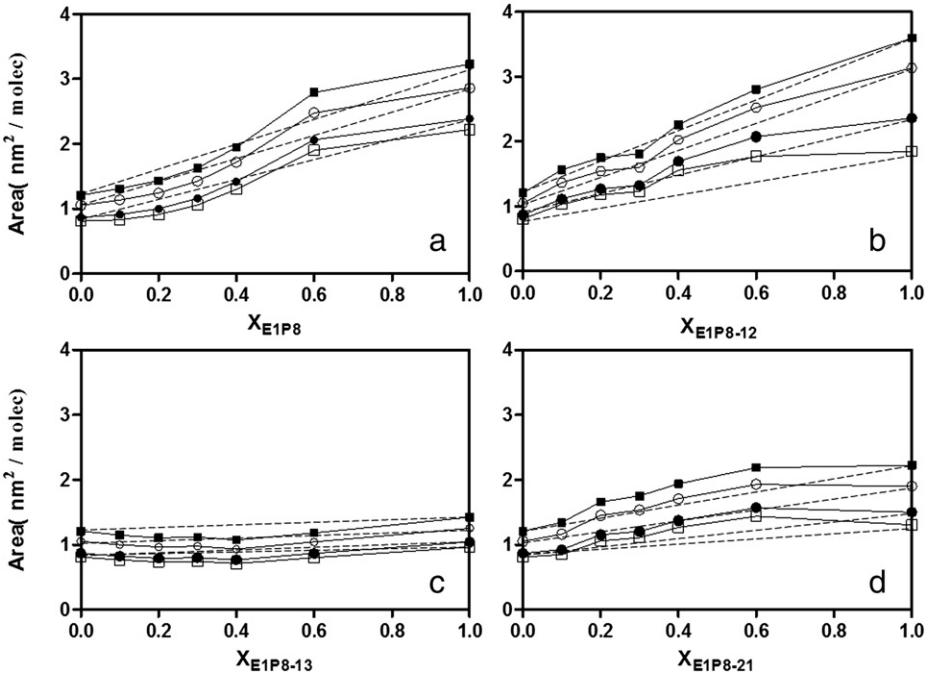

Fig. 6. Plots of area per molecule for E1P8 (a), E1P8-12 (b), E1P8-13 (c) and E1P8-21 (d) as function of the peptide mole fractions at 5 mN m^{-1} (■), 10 mN m^{-1} (○), 20 mN m^{-1} (●) and 25 mN m^{-1} (□) surface pressures for pure and mixed monolayers of POPG.

Table 3
The excess free energy of mixing (G^E) (J mol^{-1}) in mixed monolayers of E1P8, E1P8-12, E1P8-13, E1P8-21 and POPG at surface pressures 5 and 25 mN m^{-1}.

		G^E (J mol^{-1})	
		5 mN m^{-1}	25 mN m^{-1}
E1P8	0.1	666.3	960.1
	0.2	953.1	1109,6
	0.4	65.6	215,5
	0.6	−292.0	844.8
E1P8-12	0.1	137.3	−41.9
	0.2	136.1	−1016.7
	0.4	123.5	−2329.7
	0.6	13.9	−1403.4
E1P8-13	0.1	−52.3	−201.4
	0.2	−40.2	−327.5
	0.4	−411.7	−544.8
	0.6	−10.5	−386.3
E1P8-21	0.1	51.3	393.9
	0.2	5.5	791.4
	0.4	13.5	499.3
	0.6	37.7	306.6

observed (Fig. 9). In all cases, the peptides reduced the size of the domain compared with DPPG monolayers or even with DPPG monolayers containing the HIV-1 FP peptide. However, an apparent increase in the number of domains per frame maintained the average packing of the monolayer similar to that observed in the DPPG monolayers, if it is compared with that caused by HIV-1 FP. This behavior could be explained in terms of a more superficial interaction between these peptides, altering the manner in which the phase transition takes place and thus producing a larger number of nucleation sites for the formation of condensed domains but altering the overall process to a lesser extent [20,48,49]. In the case of E1P8-12, besides the above mentioned effects, a significant change in the geometry of the domains was observed. On the other hand, E1P8-13 also produced a clear effect on the total condensed phase at low pressures (see Fig. 9, at 4.3 mN m^{-1}) and led to the formation of two different green levels in the expanded liquid phase, as observed with HIV-1 FP. This result is also consistent with the observed effect of the peptide on the isotherm cited above. These differences could be explained in terms of a better interaction between E1P8-12 and E1P8-13, with the hydrophobic acyl chains of DPPG in the monolayer altering the packing rearrangement of the acyl chains of the phospholipid to a greater extent than E1P8 and E1P8-21. However, and in contrast to the behavior of HIV-1 FP, the level of condensation in the monolayer at higher pressures in the presence of E1P8-13 was similar to that observed in the presence of E1P8, E1P8-12 or E1P8-21. These would indicate that at these pressures, at which most of the phospholipid is in the condensed phase, the lateral pressure could overcome the possible effect of the substitution of a single amino acid in the sequence of the peptides, producing a behavior and perhaps an interfacial rearrangement comparable to that of E1P8 and its analogs.

3.3. E1 peptides–HIV-1 FP interactions

3.3.1. Additivity rule

In order to prove that E1P8 peptide and its analogs interact with HIV-1 FP, in addition to the *π-A* compression isotherms for POPG/E1 peptide mixtures, the *π-A* compression isotherms of mixtures of POPG/HIV-1 FP and POPG/HIV-1FP + E1 peptides (2:1) were obtained (Supplementary Material: Fig. S1). It must be pointed out that "peptide" means any of the peptide studied or mixtures of HIV-1 FP/E1 peptide (2:1). In this case each HIV-1 FP/E1 peptide (2:1) mixture is considered as one component.

The mutual interaction (attractive or repulsive) between POPG and peptide monolayers can be analyzed by examining whether the variation in area per molecule with the peptide mole fraction satisfies the additivity rule. Fig. 10 shows the area per molecule versus $X_{peptide}$ plots, at 10 mN m^{-1} surface pressure, for E1P8 (Fig. 10-a), E1P8-12 (Fig. 10-b), E1P8-13 (Fig. 10-c) and E1P8-21 (Fig. 10-d). Each plot shows a comparison between the experimental area and the estimated area based on ideal mixing (indicated by dashed lines) for each case. For the POPG/HIV-1 FP system (●), the experimental values indicated a small positive deviation with a maximum at $X_{HIV\text{-}1\ FP} = 0.2$ and 0.6. This implies the presence of a weak repulsive interaction between POPG and HIV-1 FP at low surface pressure. In the case of E1P8, E1P8-12 and E1P8-21, as indicated above, for $X_{peptide}$ ranging from 0.2

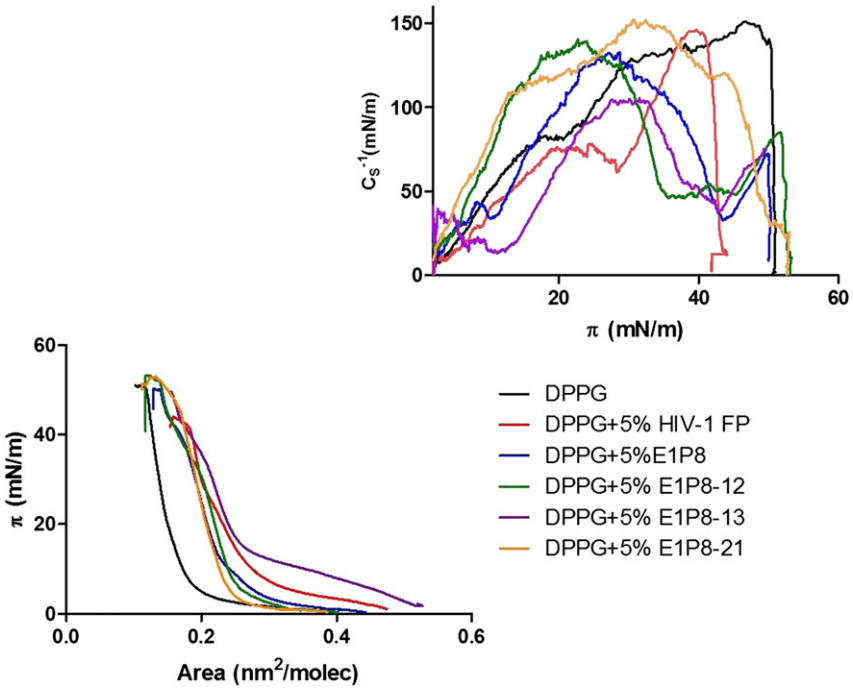

Fig. 7. Surface pressure–mean area per molecule plot for DPPG, DPPG + 5% of HIV-1 FP, DPPG + 5% of E1P8, DPPG + 5% of E1P8-12, DPPG + 5% of E1P8-13 and DPPG + 5% of E1P8-2. Inset: Plots of surface compression modulus (Cs^{-1}) as a function of the surface pressure.

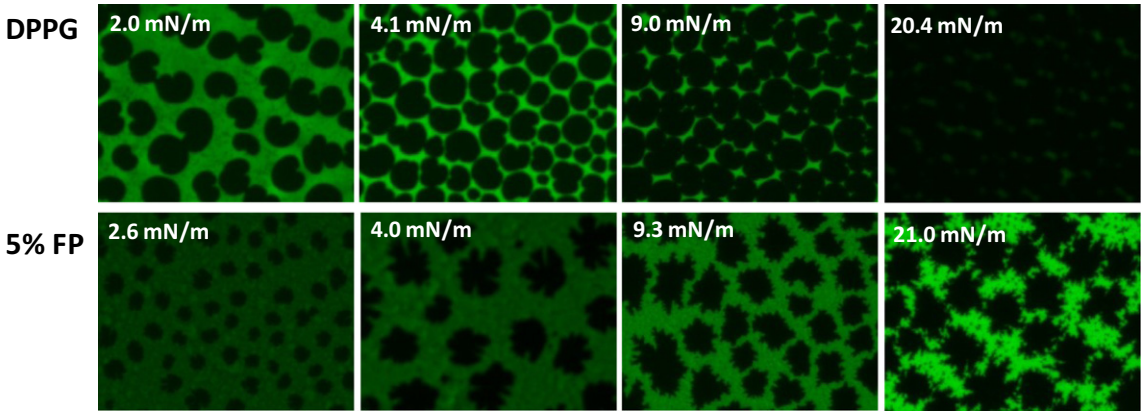

Fig. 8. FM images from DPPG monolayers with or without 5% of HIV-1 FP. Images were taken at positions matching that indicate surface pressure from LB films transferred during continuous compression. Image size: 129.5 μm × 99.8 μm.

to 0.6, the experimental values indicated smaller positive deviations than for HIV-1 FP. At $X_{peptide}$ of <0.2 and >0.6 the behavior is almost ideal. E1P8-13 follows the additivity rule as shown in Fig. 10-c (■). Finally, when a system of POPG and a mixture of HIV1-FP: E1 peptide (2:1) (▲) (as indicated above the mixture of peptides is considered as one component) was compressed slight negative deviations were observed for E1P8 between $X_{E1P8} = 0.1$ and 0.4, with positive deviations at $X_{E1P8} > 0.4$. For the E1P8-12 and E1P8-21 systems, the experimental values were consistent with the theoretical values at all mole fractions.

Although the deviations from ideality were weak, it is interesting to analyze the relative deviations caused by HIV-1 FP, and the HIV-1 FP/E1 peptide (2:1) mixtures. Fig. 11 shows the area per molecule versus surface pressure at $X_{peptide} = 0.2$. HIV-1 FP produced the largest POPG expansion monolayer indicating an interaction, according to the leakage results. When the E1 peptides were added, the expansion was reduced by half in the case of E1P8-12 and E1P8-13 and completely in the case of E1P8 and E1P8-21. So, it seems that HIV-1 FP and the E1P8 analogs interact to some extent, and that to explain the changes observed at the membrane level the peptide/peptide interaction must be taken into consideration.

3.3.2. Fluorescence microscopy

The effects of GBV-C E1P8 peptide and its analogs on the interaction between HIV-1 FP and DPPG were analyzed by performing Langmuir–Blodgett monolayer studies.

Fig. 12 shows the isotherms of DPPG alone and in the presence of 5 mol% of HIV-1 FP and different mixtures of HIV-1 FP/E1P8 derivative peptides (1:2 mol/mol). In all cases, the isotherm is shifted to even larger areas than that observed for any of the separate peptides. This behavior could indicate a dramatic change how peptides, HIV-1 FP and/or E1P8 analogs interact with each other or with DPPG in the interface. Only the HIV-1 FP/E1P8 mixture showed similar areas per

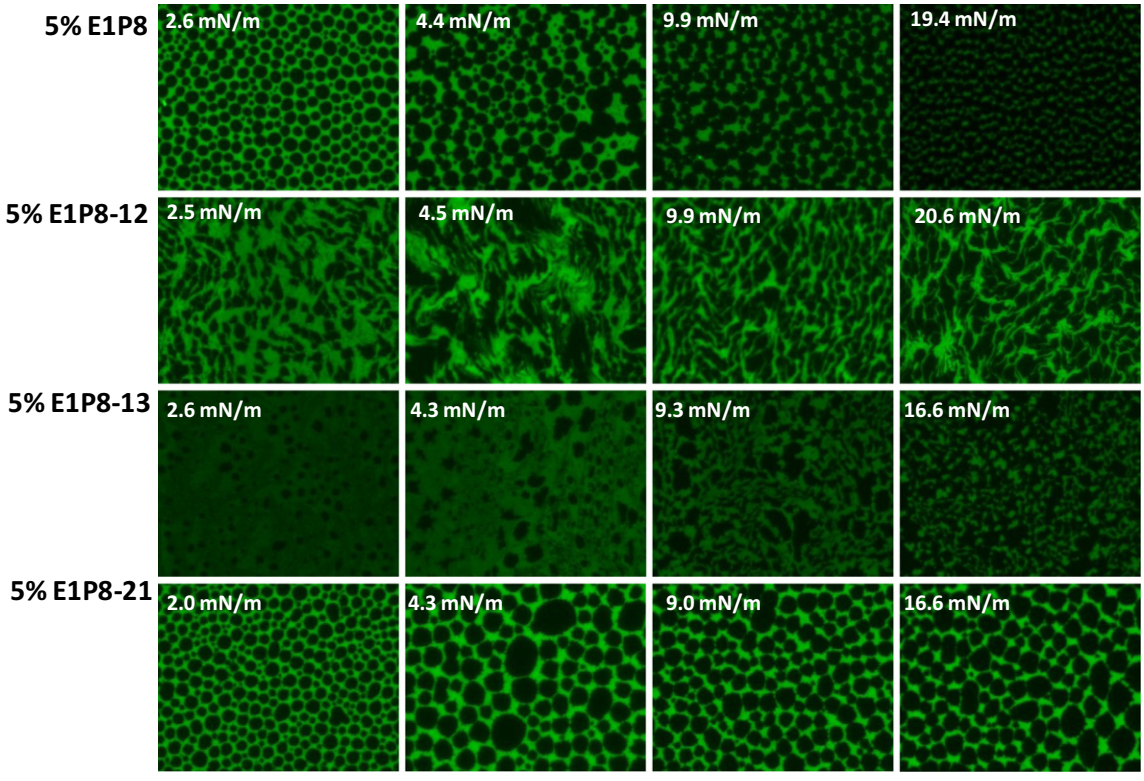

Fig. 9. FM images from DPPG monolayers with or without 5% of E1P8, E1P8-12, E1P8-13 and E1P8-21. Images were taken at positions matching that indicate surface pressure from LB films transferred during continuous compression. Image size: 129.5 μm × 99.8 μm.

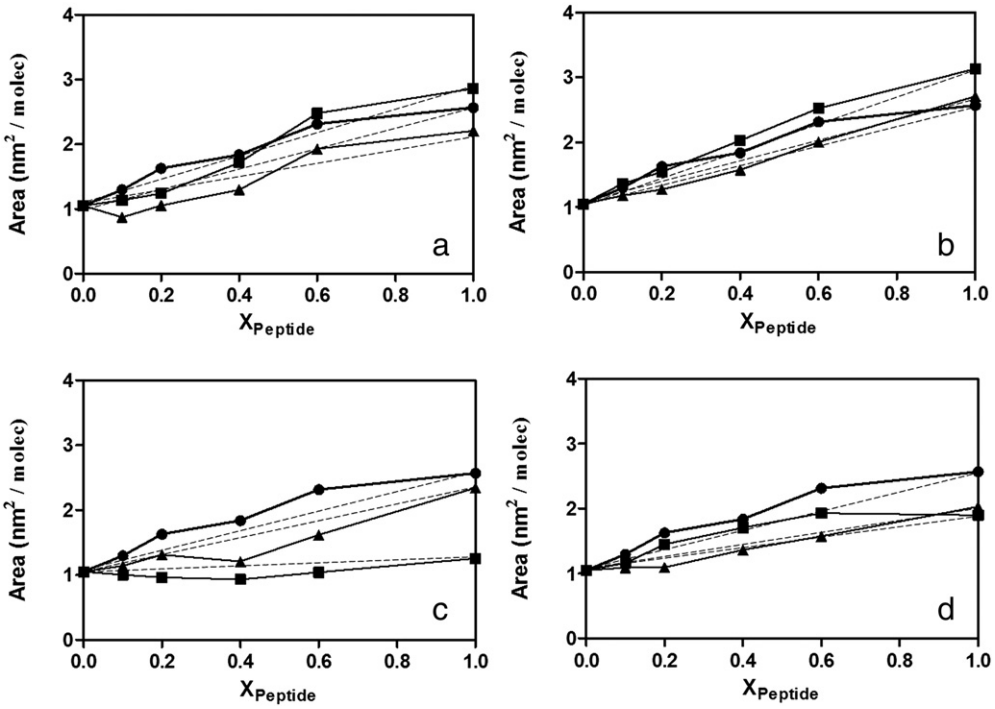

Fig. 10. Plots of *area–$X_{peptide}$* for mixtures of POPG–peptide at 10 mN m^{-1} surface pressure. a: E1P8 (■), HIV-1 FP (●), E1P8/HIV-1 FP (2:1) (▲); b: E1P8-12 (■), HIV-1 FP (●) and E1P8-12/HIV-1 FP (2:1) (▲); c: E1P8-13 (■), HIV-1 FP (●), E1P8-13/HIV-1 FP (2:1) (▲); d: E1P8-21 (■), HIV-1 FP (●), E1P8/HIV-1 FP (2:1) (▲).

molecule to those observed in each of the DPPG isotherms containing separate peptides. None of the mixtures showed significant differences in the shape of the isotherm at pressures close to the phase transition of DPPG with respect to the lipid alone, as it can be seen in Fig. 12-inset.

To further characterize the effect of the mixture of peptides on the lateral phase transition of DPPG, the monolayers containing 1 mol% of the fluorescent dye NBD-PC were observed by FM, with the appearance of dark domains of condensed phase at the interface that excluded the fluorescent dye. Fig. 13 shows images of the effect produced by the different mixtures in DPPG monolayers. Surprisingly, the behavior of the three peptides was comparable for the four combinations. All of them seemed to cancel the clear effect of HIV-1 FP on the phase transition of DPPG, showing domains with shapes and sizes similar to that observed in DPPG monolayers. The presence of HIV-1 FP also altered the behavior of EP8-12 and E1P8-13. When these peptides were added to the monolayer together with HIV-1 FP, the images obtained also showed domains with geometry and distribution similar to DPPG alone, in contrast with the shapes and the distribution observed when both peptides were included independently in the interfacial monolayer. Although the behavior observed for the different peptide combinations cannot be explained in terms of the total exclusion of HIV-1 FP from the monolayer, it is possible that the simultaneous presence of HIV-1 FP and the peptides derived from E1P8 could produce a change as HIV-1 FP when interacts with the monolayer, possibly from a relatively deep character to a more peripheral disposition. The same effect could make E1P8-12 and E1P8-13 in a comparable way to E1P8 and E1P8-21 in the presence of HIV-1 FP.

3.3.3. AFM imaging

To gain insight in the molecular organization of the interaction between lipid monolayer and the peptides studied we carry out AFM observations at two surface pressures. In this case, as indicated above, a DPPC/DPPG (2:1) mixture was used as a model membrane.

Fig. 14 shows results of DPPC/DPPG (2:1) and DPPC/DPPG (2:1)/peptides LB films transferred from air-water interface on mica substrate at 6 mN m^{-1} where, as previously reported [51,52], at room temperature DPPC and DPPG isotherms are characterized by a shoulder where LC and LE coexist. This is the case for DPPC/DPPG (2:1) monolayer at 6 mN m^{-1}.

The morphology of DPPC/DPPG (2:1) LB film is shown in Fig. 14-A (5 μm × 5 μm) and Fig. 14-a (1 μm × 1 μm), it can be seen irregular LC lipid domains (bright areas) and LE regions (dark areas). In Fig. 14-a it is possible to see the mica substrate because of imperfections

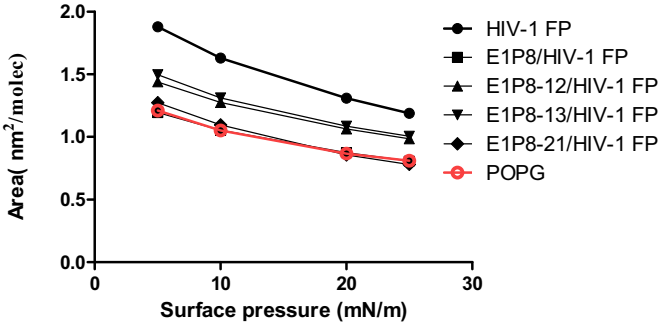

Fig. 11. Mean molecular area increase in front of surface pressure increase of mixture of POPG with HIV-1 FP, E1P8/HIV-1 FP, E1P8-12/HIV-1 FP, E1P8-13/HIV-1 FP and E1P8-21/HIV-1 FP, at molar fraction of peptides 0.2.

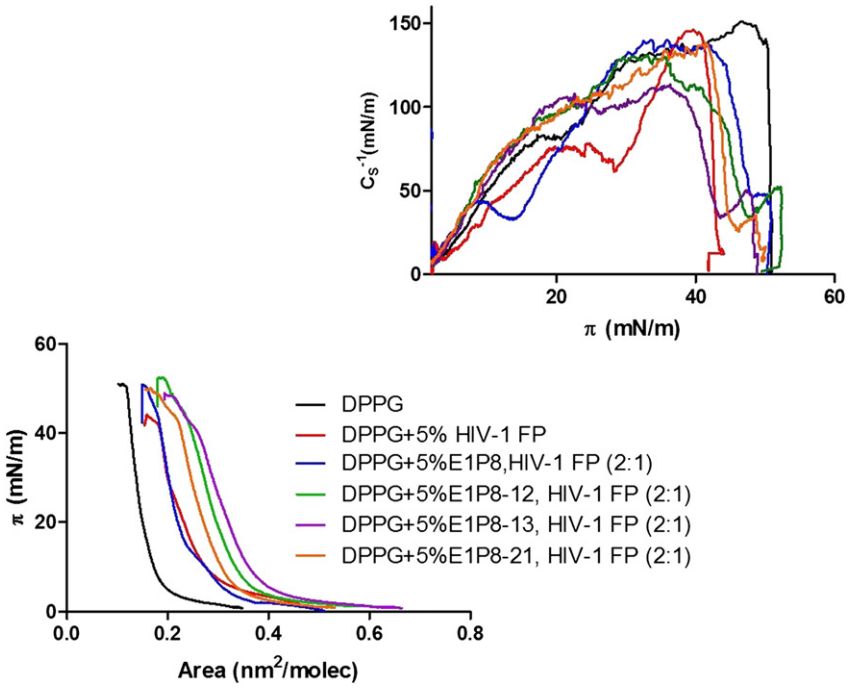

Fig. 12. Surface pressure-mean area per molecule (π-A) compression isotherms of DPPG with 5% of HIV-1 FP/E1P8, HIV-1 FP/E1P8-12, HIV-1 FP/E1P8-13 and HIV-1 FP/E1P8-21. Inset: Plots of surface compression modulus (Cs^{-1}) as a function of the surface pressure.

in LB film formation, this fact allows to differentiate the two lipid phases.

The presence of 5% E1 peptides (E1P8, E1P8-12, E1P8-13 and E1P8-21) in the monolayer altered considerably the membrane morphology. Consistent with the molecular hydrophobicity of the peptides (see Fig. 1), all of them displayed the same abilities to change lipid domains. Fig. 14-B and -b show the results obtained for the adsorption of E1P8 in the DPPC/DPPG (2:1) monolayer (images for E1P8 derivatives are supplied in the supplementary material Fig. S2, Fig S3 and Fig. S4). According with published results for amphipathic peptides [53] it can be seen that E1P8 induces round big LC domains and filaments in LE phase as a net that encloses a lower LC domains

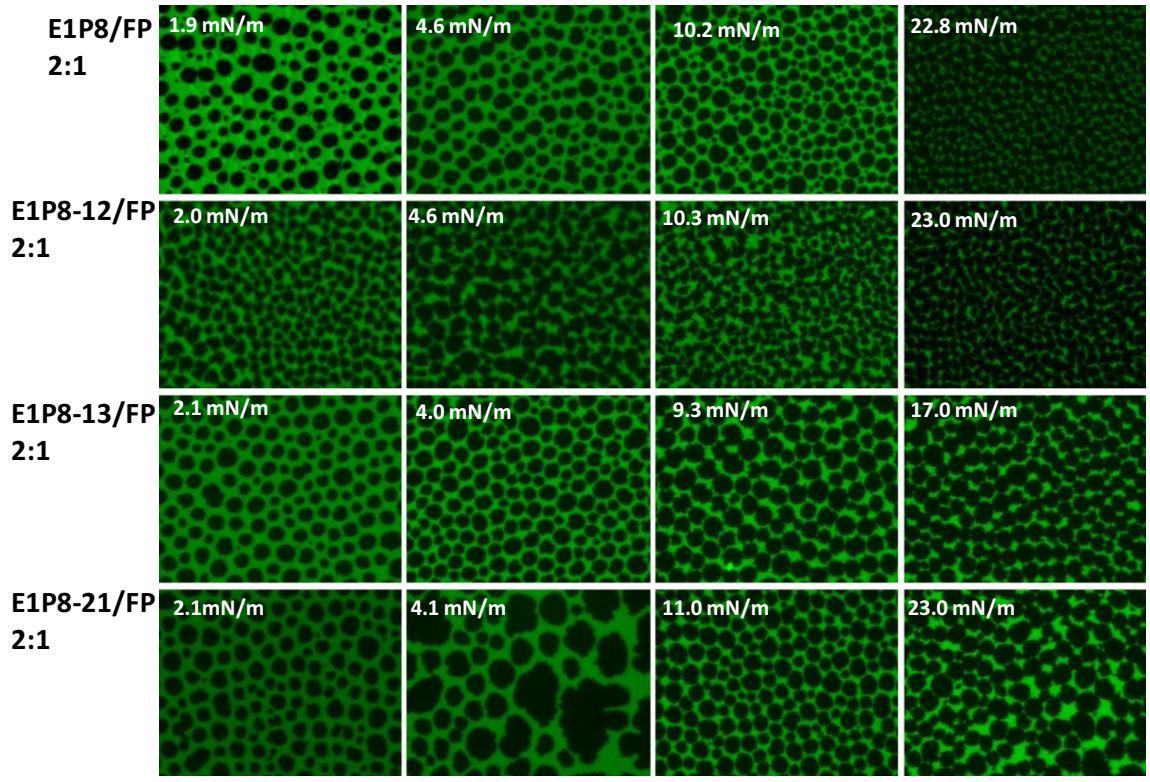

Fig. 13. FM images from DPPG monolayers with or without 5% of HIV-1 FP/E1P8, HIV-1 FP/E1P8-12, HIV-1 FP/E1P8-13 and HIV-1 FP/E1P8-21. Images were taken at positions matching that indicate surface pressure from LB films transferred during continuous compression. Image size: 129.5 μm × 99.8 μm.

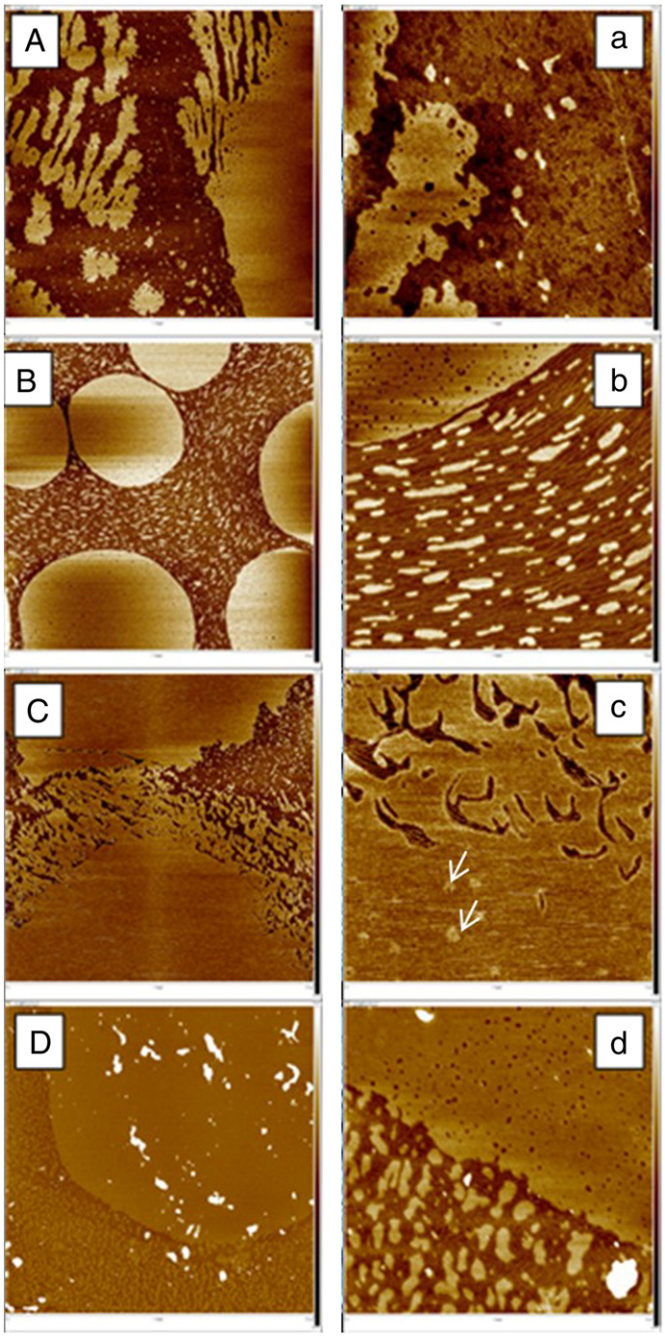

Fig. 14. AFM images for A: DPPC/DPPG (2:1), B: DPPC/DPPG (2:1) + E1P8 (5% mol), C: DPPC/DPPG (2:1) + HIV-1 FP (5% mol), D: DPPC/DPPG (2:1) + E1P8 + HIV-1 FP (2:1) (5% mol). Monolayers were transferred onto mica slides at 6 mN m^{-1}. Data scale: (A, B, C) 5 × 5 μm, (a, b, c) 1 × 1 μm. Z-scale: 4.0 nm, 4.0 nm, 1.3 nm and 5.8 nm for A, B, C and D respectively and 3.0 nm, 4.0 nm, 0.8 nm and 2.0 nm for a, b, c and d respectively.

(see Fig. 15 for details). In all images, differences in height are visible as differences in color tones. In this scale, dark brown is low and white is high.

Fig. 14-C and -c show the effect of HIV-1 FP on DPPC/DPPG (2:1) system. Also, in this case it can be seen how HIV-1 FP change LC domains but in a different way that in case of E1 peptides probably due to the net positive charge of HIV-1 FP. In this case hydrophobic interactions are less favored because of the attractive electrostatic interactions between HIV-1 FP and the anionic DPPG. The shape of LC domains dramatically changes indicating that HIV-1 FP peptide interacts preferently at the domain boundaries. On the other hand it can be seen the creation of

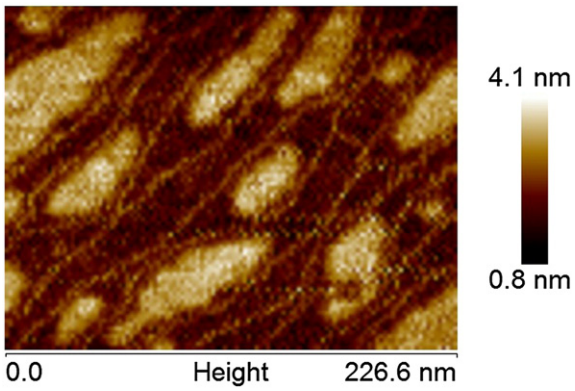

Fig. 15. AFM images for LB film composed by DPPC/DPPG (2:1) + E1P8 (5% mol). Monolayers were transferred from air–water interface onto mica slides at 6 mN m^{-1}.

nanoholes (Figs. 14-c and 16 in detail) that are agree with the fusogenic capacity of HIV-1 FP and results from leakage assay.

When HIV-1 FP and E1P8 are together in 2:1 ratio, AFM images (Fig. 14-D and -d) show also a LC-LE domain regions and also aggregates which are random distributed through the monolayer. In this case, the LB morphology is exhibited in Fig. 14-D, it can be seen a big LC domain with regular boundaries and no holes on it. Small LC domains are distributed jointly with branched filaments within LE phase.

With compression DPPC/DPPG (2:1) LB film sifts to more compact and uniform topography (Fig. 17-A and -a, which were obtained at 30 mN m^{-1} surface pressure). In addition, it can be seen the changes in the LB morphology at 30 mN m^{-1}, when peptides were added: E1P8 (5% mol) (Fig. 17-B and -b); HIV-1 FP (5% mol) (Fig. 17-C and -c) and (E1P8 + HIV-1 FP (2:1)) (5% mol) (Fig. 17-D and -d).

In case of E1P8 only few white structures are displayed. It seems that, with compression, E1P8 was excluded from the LB film according with its low capacity to penetrate anionic membranes while HIV-1 FP adopts a good structured pattern that correlate with those obtained in previous works on tilted peptides [54]. The presence of HIV-1 FP provoked the appearance of elevated domains or nanorods at the interface. Lins et al. [55] in their review "*Relationships between the*

Fig. 16. AFM image for LB film composed by DPPC/DPPG (2:1) + HIV-1 FP (5% mol). Monolayers were transferred from air–water interface onto mica slides at 6 mN m^{-1}. Data scale 1 μm × 1 μm. Z-scale: 0.5 nm. White arrows indicate nanoholes induced by HIV-1 FP peptide.

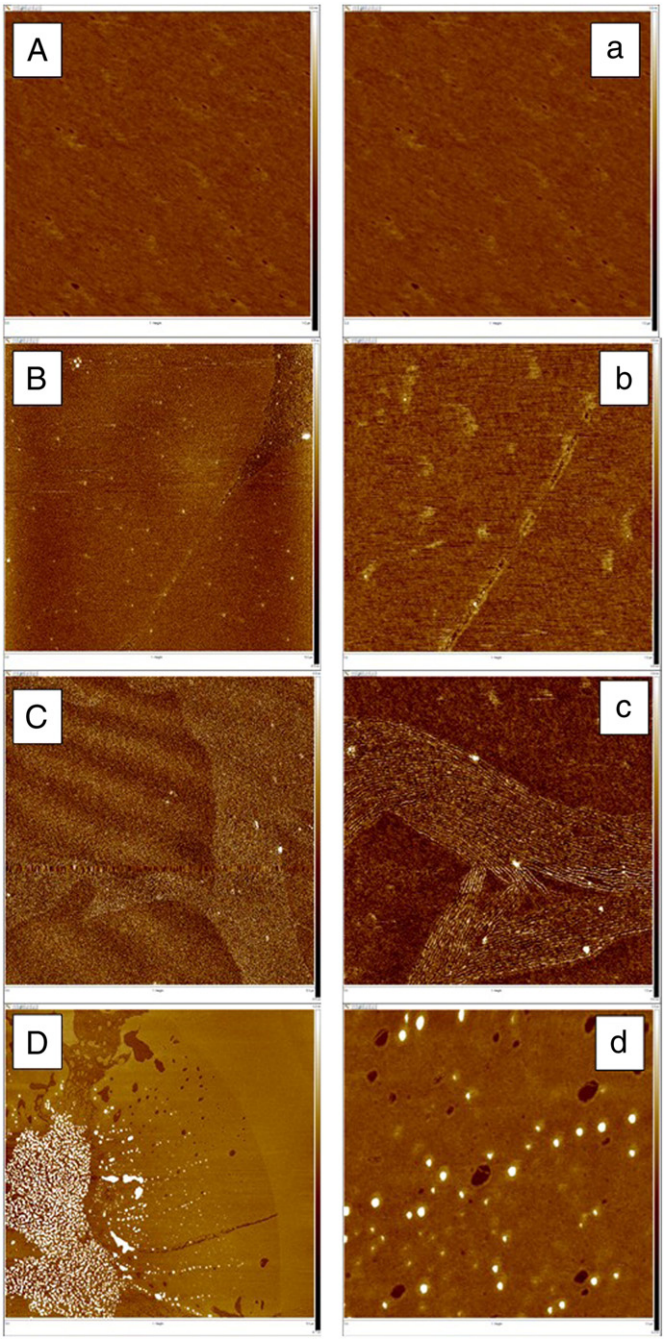

Fig. 17. AFM images for A: DPPC/DPPG (2:1), B: DPPC/DPPG (2:1) + E1P8 (5% mol), C: DPPC/DPPG (2:1) + HIV-1 FP (5% mol), D: DPPC/DPPG (2:1) + E1P8 + HIV-1 FP (2:1) (5% mol). Monolayers were transferred onto mica slides at 30 mN m^{-1}. Data scale: (A, B, C) 5 × 5 μm, (a, b, c) 1 × 1 μm. Z-scale: 4.0 nm, 0.9 nm, 0.8 nm and 3.2 nm for A, B, C and D respectively and 3.0 nm, 0.8 nm, 0.8 nm and 2.0 nm for a, b, c and d respectively.

orientation and the structural properties of peptides and their membrane interactions" suggested that these nanorods were presumably produced by the self-association of reverse cylinders made of peptides and lipids, due to the exposure of lipid tails; their association hence decreases the contact with the aqueous medium.

Fig. 17-D exhibits the dramatic change observed in DPPC/DPPG (2:1) membrane when a mixture of E1P8 + H HIV-1 FP (2:1) was added. In this case, no nanorods appeared, small round white spots are formed (probably peptide clusters or mixed lipid–peptide patches). These spots segregate out of LC domain. They show a tendency to associate. Vie et al. in their work on detection of peptide–lipid interactions in mixed monolayers [56], arrived to the conclusion that when the lipids are in the LC state (DPPC and DPPG), the general features of the AFM images reveal the existence of domains that are round for DPPG. According with this, it is possible to hypothesize that the E1P8 and HIV-1 FP first interact themselves which allow a conformational change that favours the interaction mainly with DPPG. The results demonstrate E1P8 avoid the action of HIV-1 FP at membrane level. E1P8 and HIV-1 FP peptides form compacted LB films (Fig. 18-A and -a for E1P8 peptide and Fig. 18-B and -b for HIV-1 FP) (white patches in Fig. 18-A are due to artifacts during the transfer). Images in Fig. 18-C and -c show the morphology of the LB film composed by E1P8 + HIV-1 FP (2:1), two peptides interact and arrange at the air-water interface yielding a circular structures different that those of E1PB or HIV-1 FP formed when they are alone at the interface. Similar round structures were found for others GBV-C peptides which also demonstrate their capacity to inhibit HIV-1 FP *in vitro* and *in vivo* [29].

3.3.4. Hemolysis

We compared the parent peptide and its derivative peptides (E1P8-12, E1P8-13 and E1P8-21) with regard to their capacity to inhibit the hemolytic activity of HIV-1 FP in rabbit red blood cells.

It has previously been shown [57] that the incubation of erythrocytes with highly hydrophobic, synthetic HIV-1 FP usually results in significant hemolysis.

HIV-1 FP-induced hemolysis was measured in the absence and presence of E1P8, E1P8-12, E1P8-13 and E1P8-21 peptides at different concentrations (10, 100 and 100 μM). The maximum level of HIV-1 FP-induced hemolysis (100%) is reported relative to that measured in the absence of these peptides and represents the average of three measurements.

Neither peptides nor PBS alone induced hemolysis (data not shown). Each peptide clearly inhibited HIV-1 FP hemolytic activity (Fig. 19), with hemolysis decreasing as their concentration increased. The parent peptide had a higher inhibitory effect on HIV-1 FP-induced hemolysis than its derivatives. At a molar ratio of 1:0.1 HIV-1 FP: E1 peptide (10 μM of E1P8 and its analogs), E1P8 inhibited about 80% of HIV-1 FP hemolysis, while E1P8-12 and E1P8-21 reduced HIV-1 FP hemolytic activity by around 60%, and E1P8-13 by only about 20%. The HIV-1 FP inhibitory activity of each peptide increased as their concentration increased, with total inhibition at 100 μM.

4. Conclusion

The present work offers a biophysical study of the dependence of E1P8 activity on its primary structure and its effect on HIV-1 FP action at membrane level.

Three analogs of GBV-C E1P8, in which we had replaced C^{34} and L^{35} of the peptide sequence with A and E^{24} with R, were selected. These modifications apparently enhance the anti-HIV-1 FP activity of E1P8. In fact, these GBV-C E1P8 derivatives showed an increased capacity to inhibit the leakage of POPG vesicles induced by HIV-1 FP with respect to the parent peptide [18].

The adsorption kinetics of peptides showed that the selected analogs present similar surface properties to the parent peptide, probably due to same hydrophobic profile of the peptides. The charge does not seem to be significant at this point as demonstrated by E1P8-21, in which we replaced a negative amino acid (glutamic acid) with a positive residue (arginine), which had the same activity as other peptides with a higher net negative charge. The leakage and penetration kinetics results indicate that the low interaction of the four peptides with anionic lipid is probably due to the net negative charge of the peptides and its distribution on the primary sequence, which precludes a major lipid/peptide interaction through the hydrophobic chains of the phospholipid. E1P8 and its analogs do not cause leakage and exhibit low π_e values, ranging between 10 and 19 mN m^{-1}, which confirms their inability to penetrate biological membranes.

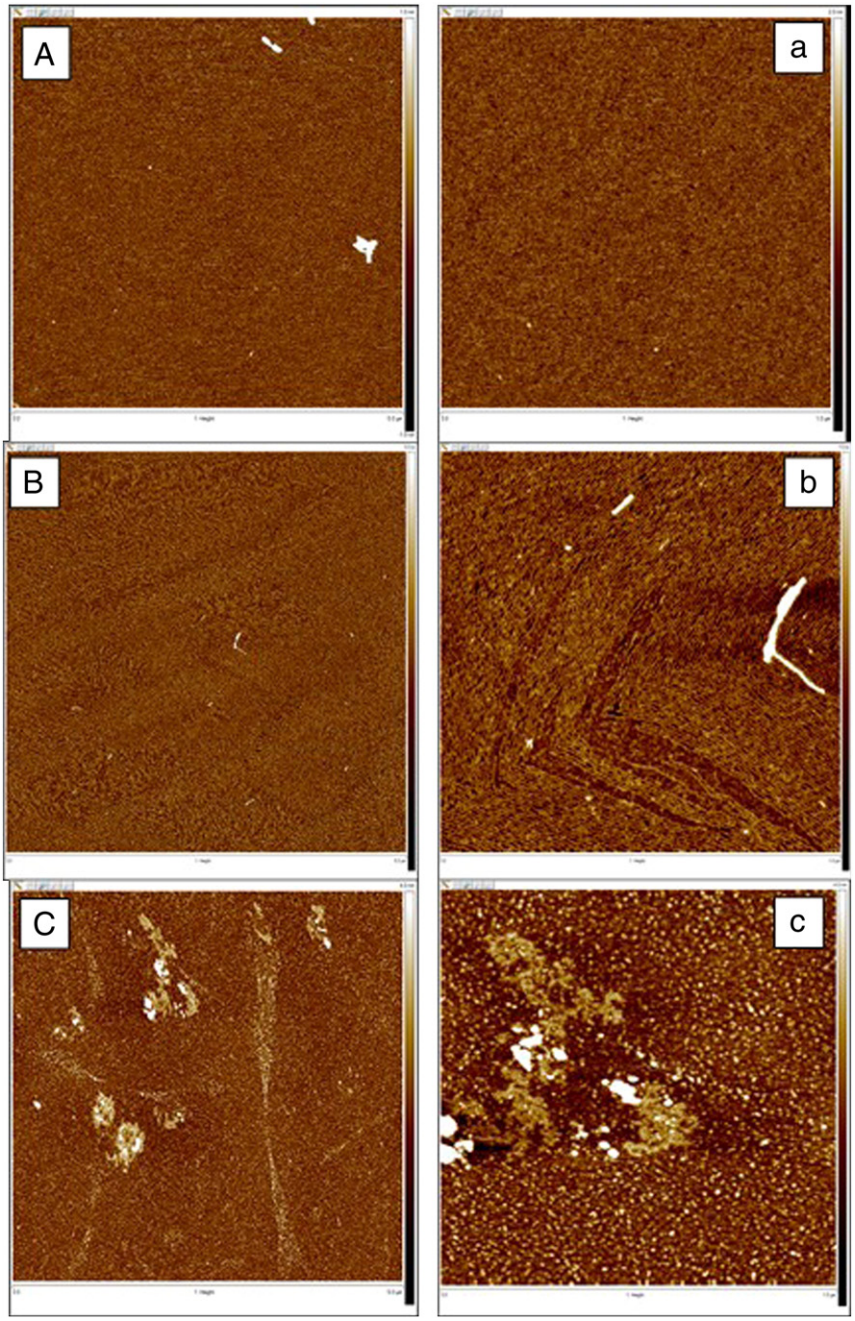

Fig. 18. AFM images for A: E1P8 GBV-C peptide monolayer, B: HIV-1 FP monolayer, C: monolayer of a mixture of E1P8 + HIV-1 FP (2:1). All monolayers were transferred on mica slides at 6 mN m^{-1}. Data scale: (A, B, C) 5 μm × 5 μm, (a, b, c): 1 μm × 1 μm. Z-scale: 1.0 nm, 3.0 nm and 4.0 nm for A, B and C respectively and 2.0 nm, 4.0 nm and 4.0 nm for a, b, and c respectively.

The miscibility of peptide/lipid binary monolayers was systematically investigated using compression isotherms and morphological techniques (FM). The variations in collapse pressure and area per molecule values suggest that some degree of interaction because the presence of peptides leads to the expansion of the POPG monolayers, except in the case of E1P8-13, and a gradual change in π_c. These changes are likely due to the different disposition and orientation of peptides during compression and not to hydrophobic interactions. These facts together with deviations in the additivity rule and G^E values allow one to hypothesize about the partial or total immiscibility of lipid/peptide mixtures.

The results regarding HIV-1 FP/POPG and (HIV-1 FP/E1 peptides)/POPG miscibility clearly indicate a certain degree of inhibition of HIV-1 FP at the membrane level, reflecting the result obtained in a leakage assay [18].

FM images provide supporting morphological information on the binary system obtained with HIV-1 FP (5% mol) or E1 peptides (5% mol) and DPPG as the lipid component. HIV-1 FP (5%) modify LC boundaries as also demonstrated at molecular level by AFM. In turn, E1 peptides caused a reduction in size of LC domains without modify the LC/LE ratio probably due to a more superficial interaction of E1 peptides with DPPG membrane or to the more affinity of them for the LE phase as AFM revealed. FM images from mixtures of E1 peptides + HIV-1 FP (2:1) with DPPG showed domains with a geometry and distribution similar to lipid alone; it seems that E1 peptides avoid the HIV-1 FP effect at the membrane. These findings were also corroborated by AFM.

In absence of the lipid, AFM images of mixtures of E1P8 and HIV-1 FP, showed the formation of a new structure indicating the interaction between two peptides. This fact allows hypothesize that the E1P8 avoid the HIV-1 FP effect due to their mutual interaction.

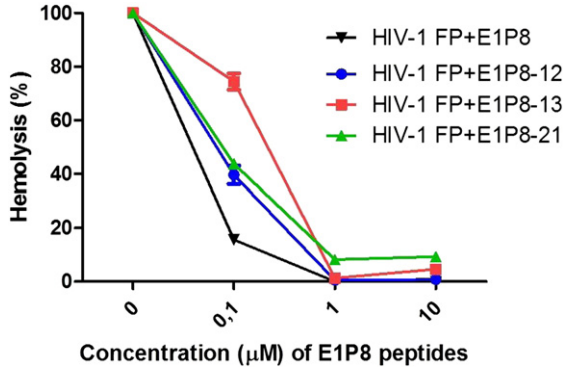

Fig. 19. % Hemolysis induced by HIV-1 FP in presence of E1P8, E1P8-12, E1P8-13 and E1P8-21 at increase concentration of E1P8 peptides.

These results were corroborated by the hemolysis study, in which all peptides inhibited the hemolytic effect of HIV-1 FP, although the extent of inhibition was dependent on peptide concentration. The best behavior in this case was shown by the E1P8 parent peptide, which drastically affected the capacity of HIV-1 FP for hemolysis, decreasing it by more than 80% at 10 μM. The combined results indicate that the changes in the primary structure of E1P8 (C^{34}, L^{35} and E^{24}) do not appear to affect its surface or hydrophobic properties, but change its behavior at the membrane level, with the expansion of the POPG monolayer becoming negligible in the case of E1P8-13 (L^{35}). The combined effect of HIV-1 FP and the E1 peptides also supported this hypothesis, as mixtures of HIV-1 FP + E1P8-21 (E^{24}) and HIV-1 FP + E1P8 did not alter the area per molecule values of POPG. In view of these facts, along with the hemolysis results, it is rational to conclude that the replacement of residues did not improve the anti HIV-1 FP activity of E1P8. Future efforts to develop new forms of E1P8 peptide should bear this in mind. Our current research is now focusing on the design of new E1P8 derivatives in which the primary structure remains unaltered, for example, by creating a cyclic peptide through a disulfide link between two cysteines.

Acknowledgments

This work was supported by research projects (CTQ2009-13969-C01, CTQ2009-13969-C02 and CTQ2012-37589C-01, CTQ2012-37589C-02) from the Secretaría de Estado de Investigación, Ministerio de Ciencia e Innovación, Dirección General de Programas y transferencia de conocimiento, Subdirección General de Proyectos de Investigación (Spain). Ramona Galatola is a recipient of a jae-PRE program pre-doctoral grant. The authors are members of the consolidated research group recognized by the Generalitat de Catalunya "Peptides and Proteins: Physicochemical Studies" (2009SGR00560).

Appendix A. Supplementary data

Supplementary data to this article can be found online at http://dx.doi.org/10.1016/j.bbamem.2014.10.033.

References

[1] P.M. Polgreen, J. Xiang, Q. Chang, J.T. Stapleton, GB virus type C/hepatitis G virus: a non-pathogenic flavivirus associated with prolonged survival in HIV-infected individuals, Microbes Infect. 5 (2003) 1255–1261.
[2] M.D. Berzsenyi, D.S. Bowden, S.K. Roberts, GB virus C: insights into co-infection, J. Clin. Virol. 33 (2005) 257–266.
[3] T. Kaiser, H.L. Tillmann, GB virus C infection: is there a clinical relevance for patients infected with the human immunodeficiency virus? AIDS Rev. 7 (2005) 3–12.
[4] J.T. Stapleton, GB virus type C/hepatitis G virus, Semin. Liver Dis. 23 (2003) 137–148.
[5] N. Bhattarai, J.T. Stapleton, GB virus C: the good boy virus? Trends Microbiol. 20 (2012) 124–130.
[6] Y. Koedel, K. Eissmann, H. Wend, B. Fleckenstein, H. Reil, Peptides derived from a distinct region of GB virus c glycoprotein E2 mediate strain-specific HIV-1 entry inhibition, J. Virol. 85 (2011) 7037–7047.
[7] S. Jung, M. Eichenmüller, N. Donhauser, F. Neipel, A.M. Engel, G. Hess, B. Fleckenstein, H. Reil, HIV entry inhibition by the envelope 2 glycoprotein of GB virus C, AIDS 21 (2007) 645–647.
[8] Q. Chang, J.H. McLinden, J.T. Stapleton, M.A. Sathar, J. Xiang, Expression of GB virus C NS5A protein from genotypes 1, 2, 3 and 5 and a 30 aa NS5A fragment inhibit human immunodeficiency virus type 1 replication in a CD4+ T-lymphocyte cell line, J. Gen. Virol. 88 (2007) 3341–3346.
[9] J. Xiang, J.H. McLinden, Q. Chang, T.M. Kaufman, J.T. Stapleton, An 85-aa segment of the GB virus type C NS5A phosphoprotein inhibits HIV-1 replication in CD4+ Jurkat T cells, Proc. Natl. Acad. Sci. U. S. A. 103 (2006) 15570–15575.
[10] J. Xiang, J.H. McLinden, R.A. Rydze, Q. Chang, T.M. Kaufman, D. Klinzman, J.T. Stapleton, Viruses within the Flaviviridae decrease CD4 expression and inhibit HIV replication in human CD4+ cells, J. Immunol. 183 (2009) 7860–7869.
[11] E. Herrera, S. Tenckhoff, M.J. Gómara, R. Galatola, M.J. Bleda, C. Gil, G. Ercilla, J.M. Gatell, H.L. Tillmann, I. Haro, Effect of synthetic peptides belonging to E2 envelope protein of GB virus C on human immunodeficiency virus type 1 infection, J. Med. Chem. 53 (2010) 6054–6063.
[12] M.J. Sánchez-Martín, J.M. Amigo, M. Pujol, I. Haro, M.A. Alsina, M.A. Busquets, Fluorescence study of the dynamic interaction between E1(145-162) sequence of hepatitis GB virus C and liposomes, Anal. Bioanal. Chem. 394 (2009) 1003–1010.
[13] M.J. Sánchez-Martín, M.A. Busquets, V. Girona, I. Haro, M.A. Alsina, M. Pujol, Effect of E1(64-81) hepatitis G peptide on the in vitro interaction of HIV-1 fusion peptide with membrane models, BBA - Biomembr. 1808 (2011) 2178–2188.
[14] M.J. Sánchez-Martín, A. Cruz, M.A. Busquets, I. Haro, M.A. Alsina, M. Pujol, Physico-chemical characterization of GBV-C E1 peptides as potential inhibitors of HIV-1 fusion peptide: interaction with model membranes, Int. J. Pharm. 436 (2012) 593–601.
[15] M.J. Sánchez-Martin, I. Haro, M.A. Alsina, M.A. Busquets, M. Pujol, A langmuir monolayer study of the interaction of E1(145-162) hepatitis G virus peptide with phospholipid membranes, J. Phys. Chem. B 114 (2010) 448–456.
[16] M.J. Sánchez-Martín, K. Hristova, M. Pujol, M.J. Gómara, I. Haro, M. Asunción Alsina, M. Antònia Busquets, Analysis of HIV-1 fusion peptide inhibition by synthetic peptides from E1 protein of GB virus C, J. Colloid Interface Sci. 360 (2011) 124–131.
[17] M.J. Sánchez-Martín, P. Urbán, M. Pujol, I. Haro, M.A. Alsina, M.A. Busquets, Biophysical investigations of GBV-C E1 peptides as potential inhibitors of HIV-1 fusion peptide, ChemPhysChem 12 (2011) 2816–2822.
[18] R. Galatola, M.J. Gómara, M. Escarrà, M.J. Bleda, M. Pujol, M.A. Alsina, I. Haro, Study of the interaction between the HIV-1 fusion peptide and E1/E2 GB virus c derived peptides in XV International Symposium on Luminescence Spectrometry—Biophysical and Analytical Aspects, Extended Abstracts, 19-22 June 2012, Barcelona, Spain - (ISLS 2012), Luminescence 27 (2012) 534–572.
[19] L. Wang, A. Cruz, C.R. Flach, J. Pérez-Gil, R. Mendelsohn, Langmuir–Blodgett films formed by continuously varying surface pressure. Characterization by IR spectroscopy and epifluorescence microscopy, Langmuir 23 (2007) 4950–4958.
[20] A. Cruz, L.A. Worthman, A.G. Serrano, C. Casals, K.M.W. Keough, J. Pérez-Gil, Microstructure and dynamic surface properties of surfactant protein SP-B/dipalmitoylphosphatidylcholine interfacial films spread from lipid-protein bilayers, Eur. Biophys. J. 29 (2000) 204–213.
[21] H. Ellens, J. Bentz, F.C. Szoka, H^+- and Ca^{2+}-induced fusion and destabilization of liposomes, Biochemistry 24 (1985) 3099–3106.
[22] M. Smolarsky, D. Teitelbaum, M. Sela, C. Gitler, A simple fluorescent method to determine complement mediated liposome immune lysis, J. Immunol. Methods 15 (1977) 255–265.
[23] C. Larios, J. Casas, M.A. Alsina, C. Mestres, M.J. Gómara, I. Haro, Characterization of a putative fusogenic sequence in the E2 hepatitis G virus protein, Arch. Biochem. Biophys. 442 (2005) 149–159.
[24] M. Rafalski, J.D. Lear, W.F. DeGrado, Phospholipid interactions of synthetic peptides representing the N-terminus of HIV gp41, Biochemistry 29 (1990) 7917–7922.
[25] C. Larios, J. Miñones Jr., I. Haro, M.A. Alsina, M.A. Busquets, J. Miñones Trillo, Study of adsorption and penetration of E2(279-298) peptide into langmuir phospholipid monolayers, J. Phys. Chem. B 110 (2006) 23292–23299.
[26] E.E. Ambroggio, F. Separovic, J. Bowie, G.D. Fidelio, Surface behaviour and peptide–lipid interactions of the antibiotic peptides, Maculatin and Citropin, BBA - Biomembr. 1664 (2004) 31–37.
[27] A. Won, S. Pripotnev, A. Ruscito, A. Ianoul, Effect of point mutations on the secondary structure and membrane interaction of antimicrobial peptide anoplin, J. Phys. Chem. B 115 (2011) 2371–2379.
[28] S.R. Dennison, D.A. Phoenix, Influence of C-terminal amidation on the efficacy of modelin-5, Biochemistry 50 (2011) 1514–1523.
[29] I. Haro, M.J. Gómara, R. Galatola, O. Domenech, J. Prat, V. Girona, M.A. Busquets, Study of the inhibition capacity of an 18-mer peptide domain of GBV-C virus on gp41-FP HIV-1 activity, BBA - Biomembr. 1808 (2011) 1567–1573.
[30] T.P. Hopp, K.R. Woods, Prediction of protein antigenic determinants from amino acid sequences, Proc. Natl. Acad. Sci. 78 (1981) 3824–3828.
[31] M.J. Gómara, M. Lorizate, N. Huarte, I. Mingarro, E. Perez-Payá, J.L. Nieva, Hexapeptides that interfere with HIV-1 fusion peptide activity in liposomes block GP41-mediated membrane fusion, FEBS Lett. 580 (2006) 2561–2566.
[32] E. Eiriksdottir, K. Konate, Ü. Langel, G. Divita, S. Deshayes, Secondary structure of cell-penetrating peptides controls membrane interaction and insertion, BBA - Biomembr. 1798 (2010) 1119–1128.
[33] M.A. Alsina, A. Ortiz, D. Polo, F. Comelles, F. Reig, Synthesis and study of molecular interactions between phosphatidyl choline and two laminin derived peptides hydrophobically modified, J. Colloid Interface Sci. 294 (2006) 385–390.

[34] R. Maget-Dana, The monolayer technique: a potent tool for studying the interfacial properties of antimicrobial and membrane-lytic peptides and their interactions with lipid membranes, BBA - Biomembr. 1462 (1999) 109–140.
[35] P. Bougis, H. Rochat, G. Piéroni, R. Verger, Penetration of phospholipid monolayers by cardiotoxins, Biochemistry 20 (1981) 4915–4920.
[36] K. Tsumoto, H. Matsuo, M. Tomita, T. Yoshimura, Efficient formation of giant liposomes through the gentle hydration of phosphatidylcholine films doped with sugar, Colloids Surf. B: Biointerfaces 68 (2009) 98–105.
[37] D. Marsh, Lateral pressure in membranes, BBA - Rev. Biomembr. 1286 (1996) 183–223.
[38] R. Maget-Dana, D. Lelivre, Comparative interaction of α-helical and β-sheet amphiphilic isopeptides with phospholipid monolayers, Biopolymers 59 (2001) 1–10.
[39] J.T. Davies, G.R.A. Mayers, The effect of interfacial films on mass transfer rates in liquid-liquid extraction, Chem. Eng. Sci. 16 (1961) 55–68.
[40] D.K. Chattoraj, K.S. Birdi, Adsortion and the Gibbs Surface Excess, Plenum Press, New York, 1984. 219–222.
[41] F. Takeda, M. Matsumoto, T. Takenaka, Y. Fujiyoshi, N. Uyeda, Surface pressure dependence of monolayer structure of poly-ε{lunate}-benzyloxycarbonyl-l-lysine, J. Colloid Interface Sci. 91 (1983) 267–271.
[42] M. Kaku, H. Hsiung, D.Y. Sogah, M. Levy, J.M. Rodríguez-Parada, Monolayers and Langmuir–Blodgett films of poly(N-acylethylenimines), Langmuir 8 (1992) 1239–1242.
[43] K. Hac-Wydro, J. Kapusta, A. Jagoda, P. Wydro, P. Dynarowicz-Łatka, The influence of phospholipid structure on the interactions with nystatin, a polyene antifungal antibiotic. A Langmuir monolayer study, Chem. Phys. Lipids 150 (2007) 125–135.
[44] L. Picas, C. Suárez-Germà, M.T. Montero, O. Domènech, J. Hernández-Borrell, Miscibility behavior and nanostructure of monolayers of the main phospholipids of escherichia coli inner membrane, Langmuir 28 (2012) 701–706.
[45] K.Y.C. Lee, Collapse mechanisms of langmuir monolayers, 592008. 771–791.
[46] R.E. Pagano, N.L. Gershfeld, A millidyne film balance for measuring intermolecular energies in lipid films, J. Colloid Interface Sci. 41 (1972) 311–317.
[47] G.L. Gaines, Insoluble Monolayers at Liquid–Gas Interface, Wiley-Interscience, New York, 1966. 286.
[48] K. Nag, J. Perez-Gil, A. Cruz, K.M.W. Keough, Fluorescently labeled pulmonary surfactant protein C in spread phospholipid monolayers, Biophys. J. 71 (1996) 246–256.
[49] K. Nag, S.G. Taneva, J. Perez-Gil, A. Cruz, K.M.W. Keough, Combinations of fluorescently labeled pulmonary surfactant proteins SP- B and SP-C in phospholipid films, Biophys. J. 72 (1997) 2638–2650.
[50] D. Lukovic, A. Cruz, A. Gonzalez-Horta, A. Almlen, T. Curstedt, I. Mingarro, J. Pérez-Gil, Interfacial behavior of recombinant forms of human pulmonary surfactant protein SP-C, Langmuir 28 (2012) 7811–7825.
[51] H. Nakahara, S. Nakamura, S. Lee, G. Sugihara, O. Shibata, Influence of a new amphiphilic peptide with phospholipid monolayers at the air–water interface, Colloids Surf. A Physicochem. Eng. Asp. 270–271 (2005) 52–60.
[52] J.A. Castillo, A. Pinazo, J. Carilla, M.R. Infante, M.A. Alsina, I. Haro, P. Clapés, Interaction of antimicrobial arginine-based cationic surfactants with liposomes and lipid monolayers, Langmuir 20 (2004) 3379–3387.
[53] H.A. Rinia, R.A. Kik, R.A. Demel, M.M.E. Snel, J.A. Killian, J.P.J.M. van der Eerden, B. de Kruijff, Visualization of highly ordered striated domains induced by transmembrane peptides in supported phosphatidylcholine bilayers, Biochemistry 39 (2000) 5852–5858.
[54] K. El Kirat, L. Lins, R. Brasseur, Y.F. Dufrêne, Fusogenic tilted peptides induce nanoscale holes in supported phosphatidylcholine bilayers, Langmuir 21 (2005) 3116–3121.
[55] L. Lins, A. Thomas, R. Brasseur, Relationships between the orientation and the structural properties of peptides and their membrane interactions, BBA - Biomembr. 1778 (2008) 1537–1544.
[56] V. Vié, N. Van Mau, L. Chaloin, E. Lesniewska, C. Le Grimellec, F. Heitz, Detection of peptide–lipid interactions in mixed monolayers, using isotherms, atomic force microscopy, and Fourier transform infrared analyses, Biophys. J. 78 (2000) 846–856.
[57] P.W. Mobley, C.C. Curtain, a. Kirkpatrick, M. Rostamkhani, A.J. Waring, L.M. Gordon, The amino-terminal peptide of HIV-1 glycoprotein 41 lyses human erythrocytes and CD4+ lymphocytes, BBA - Mol. Basis Dis. 1139 (1992) 251–256.